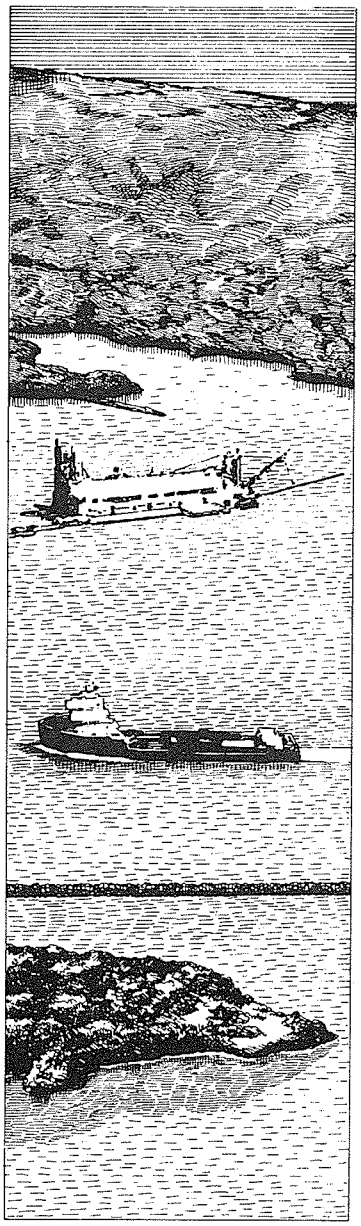

DREDGING RESEARCH PROGRAM

TECHNICAL REPORT DRP-92-8

PRELIMINARY DESIGN FOR DREDGED MATERIAL PLACEMENT PHYSICAL MODELING FACILITIES

by

Mills Soldate, James R. Pagenkopf, Michael R. Morton

Tetra Tech, Inc.
1911 North Fort Myer Drive
Arlington, Virginia 22209

December 1992
Final Report

Prepared for DEPARTMENT OF THE ARMY
US Army Corps of Engineers
Washington, DC 20314-1000

Monitored by Hydraulics Laboratory
US Army Engineer Waterways Experiment Station
3909 Halls Ferry Road, Vicksburg, Mississippi 39180-6199

Under Work Unit No. 32465

The Dredging Research Program (DRP) is a seven-year program of the US Army Corps of Engineers. DRP research is managed in these five technical areas:

Area 1 - Analysis of Dredged Material Placed in Open Water

Area 2 - Material Properties Related to Navigation and Dredging

Area 3 - Dredge Plant Equipment and Systems Processes

Area 4 - Vessel Positioning, Survey Controls, and Dredge Monitoring Systems

Area 5 - Management of Dredging Projects

REPORT DOCUMENTATION PAGE

Form Approved
OMB No. 0704-0188

1. AGENCY USE ONLY (Leave blank)	2. REPORT DATE	3. REPORT TYPE AND DATES COVERED
	December 1992	Final report

4. TITLE AND SUBTITLE

Preliminary Design for Dredged Material Placement Physical Modeling Facilities

5. FUNDING NUMBERS

WU 32465

6. AUTHOR(S)

Mills Soldate
James R. Pagenkopf
Michael R. Morton

7. PERFORMING ORGANIZATION NAME(S) AND ADDRESS(ES)

Tetra Tech, Inc., 1911 North Fort Myer Drive
Arlington, VA 22209

8. PERFORMING ORGANIZATION REPORT NUMBER

9. SPONSORING/MONITORING AGENCY NAME(S) AND ADDRESS(ES)

US Army Corps of Engineers, Washington, DC 20314-1000

USAE Waterways Experiment Station, Hydraulics Laboratory
3909 Halls Ferry Road, Vicksburg, MS 39180-6199

10. SPONSORING/MONITORING AGENCY REPORT NUMBER

Technical Report
DRP-92-8

11. SUPPLEMENTARY NOTES

Available from National Technical Information Service, 5285 Port Royal Road, Springfield, VA 22161.

12a. DISTRIBUTION/AVAILABILITY STATEMENT

Approved for public release; distribution is unlimited

12b. DISTRIBUTION CODE

13. ABSTRACT *(Maximum 200 words)*

The feasibility of performing laboratory experiments to aid in the modification and enhancement of existing numerical models for predicting the physical fate of dredged material discharged into open water is addressed. First, appropriate scaling laws are investigated to determine if prototype dredged material disposal behavior can be accurately simulated in a physical test facility for various cohesive and noncohesive sediments. Information gained from this investigation is used to determine the general design requirements of the test facility. These requirements include the types of equipment and measurement techniques required to monitor rates of cloud entrainment, rates of spreading on the bottom, disposal material properties, suspended sediment concentrations, and other parameters of interest. Typical testing scenarios for various discharge conditions are included.

14. SUBJECT TERMS		15. NUMBER OF PAGES
Disposal	Modeling	55
Dredged material	Scaling laws	16. PRICE CODE
Dredging	Sediment	

17. SECURITY CLASSIFICATION OF REPORT	18. SECURITY CLASSIFICATION OF THIS PAGE	19. SECURITY CLASSIFICATION OF ABSTRACT	20. LIMITATION OF ABSTRACT
UNCLASSIFIED	UNCLASSIFIED		

PREFACE

The work described in this report was performed under Contract No. DACW39-87-D-0028, titled "Preliminary Design for Dredged Material Disposal Modeling Facilities," between the US Army Engineer Waterways Experiment Station (WES), Vicksburg, MS, and Tetra Tech, Inc., Pasadena, CA. This study was sponsored by the Headquarters, US Army Corps of Engineers (HQUSACE), under Dredging Research Program (DRP) Work Unit No. 32465, "Numerical Simulation Techniques for Evaluation of Short-Term Fate and Stabilization of Dredged Material Disposal in Open Waters," and monitored by the Hydraulics Laboratory (HL), WES. HQUSACE Technical Monitors for the DRP were Messrs. Glenn Drummond, Vince Montante, Rixie Hardy, and John Parez. HQUSACE Advisors were Messrs. M. K. Miles, Ben I. Kelly, and Don Pommer.

The study was conducted during the period January-June 1988 under the general supervision of Messrs. F. A. Herrmann, Jr., Director, HL; R. A. Sager, Assistant Director, HL; M. B. Boyd, Chief, Waterways Division, HL; and M. J. Trawle, Chief, Math Modeling Group, Waterways Division, HL. The study was performed and the report written by Dr. A. Mills Soldate, Mr. James R. Pagenkopf, and Mr. Michael R. Morton of Tetra Tech, Inc. The contract was monitored by Dr. Billy H. Johnson, Math Modeling Group, who was the Contracting Officer's Technical Representative for this study. Additional helpful contributions concerning existing facilities and equipment at WES were made by Mr. Trawle. Dr. Nicholas Kraus, Coastal Engineering Research Center, WES, was the Technical Manager for Problem Area 1, "Analysis of Dredged Materials Disposal." Mr. E. Clark McNair and Ms. Carolyn M. Holmes, Coastal Engineering Research Center, were DRP Program Manager and Assistant Program Manager, respectively. This report was edited by Mrs. Marsha C. Gay, Information Technology Laboratory, WES.

At the time of publication of this report, Director of WES was Dr. Robert W. Whalin. Commander was COL Leonard G. Hassell, EN.

Additional information on this report can be obtained from Mr. E. Clark McNair, Jr., DRP Program Manager, at (601) 634-2070.

CONTENTS

	Page
PREFACE	1
CONVERSION FACTORS, NON-SI TO SI (METRIC) UNITS OF MEASUREMENT	3
SUMMARY	4
KEY	6
PART I: INTRODUCTION	7
Background and Purpose	7
General Approach	8
PART II: INVESTIGATION OF SCALING LAWS	9
Dredged Material Disposal Methods	9
Numerical Disposal Models	9
Dredged Material Disposal Characteristics	11
Model Scaling Analysis	12
Other Scaling Considerations	27
PART III: PRELIMINARY DESIGN OF TESTING FACILITY	29
Sizing and Layout of Facility	29
Monitoring Techniques	37
Data Acquisition and Management	44
PART IV: CONCLUSIONS AND RECOMMENDATIONS	46
Conclusions	46
Recommendations	47
REFERENCES	48
TABLES 1 AND 2	
APPENDIX A: NOTATION	A1

CONVERSION FACTORS, NON-SI TO SI (METRIC) UNITS OF MEASUREMENT

Non-SI units of measurement used in this report can be converted to SI (metric) units as follows:

Multiply	By	To Obtain
cubic yards	0.02831685	cubic metres
degrees (angle)	0.01745329	radians
feet	0.3048	metres
gallons (US liquid)	3.785412	cubic decimetres
inches	0.0254	metres
knots	0.5147	metres per second
square feet	0.09290304	square metres

SUMMARY

One important aspect in determining the impact of dredging and disposal operations is determining where and how the disposal material is initially dispersed and/or deposited after discharge. Numerical models exist for predicting the short-term fate of dredged material discharged into open water. However, these models contain known deficiencies and also suffer from a lack of verification. Under Dredging Research Program (DRP) Work Unit No. 32465, "Numerical Simulation Techniques for Evaluation of Short-Term Fate and Stabilization of Dredged Material Disposal in Open Waters," controlled laboratory disposal tests are planned to aid in removing numerical model deficiencies and to provide data sets for model verification. As in any physical model testing program, scaling effects must be considered in the design of the facility.

A dimensional analysis for undistorted model disposal tests has been conducted. This analysis was performed first for the convective descent of the disposal material through the water column and then for the dynamic collapse of the disposal cloud or jet on the bottom. This analysis indicates that scaling of the prototype is possible for the convective descent phase provided that the model Reynolds number is high enough so that turbulent flow occurs. For turbulent flow, the drag coefficient is a weak function of the Reynolds number and thus similitude can be approximately attained even though Reynolds number similitude is not actually achieved. Froude number similitude is always required. Assuming that dynamic collapse occurs on the bottom, it is necessary that model and prototype Reynolds number similitude be achieved. This is possible by increasing the bottom sediment diameter.

The Reynolds number requirements put a limit on the model-to-prototype length scale that can be used. Because of the need to create turbulent flow in the model, the smallest length scale that can be employed is about 1:100. Thus, the physical model facility should be greater than 1:100 (e.g., 1:75, 1:50, etc.).

Also of importance in designing an adequate testing facility is the development of monitoring methods and monitoring equipment to allow meaningful characterization of the complex processes governing the convective descent and bottom collapse phases of the discharge and the resultant distribution of suspended and deposited sediment.

The dredged material disposal experiments will involve the measurement of a number of specific properties of interest, including the size and shape of the descending cloud or discharge jet, the rate of descent of the descending cloud, the rate of entrainment of ambient water, the vertical density profile (if applicable), the vertical and horizontal currents induced by the discharge, the rate of spreading on the bottom, the suspended sediment concentration distributions, the bottom sediment accumulation distribution, and disposal material properties. A number of types of test monitoring equipment to measure these properties are available. These include small electromagnetic velocity meters, salinity meters, video recorders, turbidimeters, and test tubes for manually sampling suspended sediment concentrations.

PRELIMINARY DESIGN FOR DREDGED MATERIAL PLACEMENT PHYSICAL MODELING FACILITIES

KEY

Manufacturer	Symbol	Product
Montedoro-Whitney Corp. San Luis Obisbo, CA	MVM-1	Miniature electromagnetic velocity meter
Montedoro-Whitney Corp. San Luis Obisbo, CA	MCM-1	Miniature temperature-conductivity meter
Downing & Associates Washington, DC	OBS-2	Optical backscatter turbidimeter
Data Translation, Inc. Marlboro, MA	DT-2851	High-resolution digital image processing frame grabber
Data Translation, Inc. Marlboro, MA	DT-IRIS	Digital image processing software library
IBM Corporation Boca Raton, FL	IBM-AT	80286-based microcomputer

PRELIMINARY DESIGN FOR DREDGED MATERIAL PLACEMENT PHYSICAL MODELING FACILITIES

PART I: INTRODUCTION

Background and Purpose

1. A series of numerical models have been developed by the US Army Engineer Waterways Experiment Station (WES) and used over the last several years to determine the short-term fate of dredged material discharged into the aquatic environment. The ability to predict the movement and fate of dredged sediments is crucial to assessing the environmental impacts of the discharge and investigating the relative merits of alternative disposal sites and discharge methods.

2. Models currently available include the original disposal models for an instantaneous dump (DMF) and for a continuous discharge (DMFJ) developed by Brandsma and Divoky (1976) as well as modified versions called DIFID (Disposal from Instantaneous Dump), DIFCD (Disposal from Continuous Discharge), and DIFHD (Disposal from Hopper Dredge) developed by Johnson (in preparation). These models have proven useful for evaluating certain discharge conditions, but require improvements to address a wider range of actual prototype discharge methods. For example, the existing models do not allow adequate simulation of moving multiple dumps (hopper dredges) or pipeline disposal with splash plates. Also, even for relatively simple discharge conditions (i.e., stationary instantaneous dumps), the models have not been thoroughly verified using field or laboratory prototype experimental data.

3. In order to improve capabilities to predict numerically the short-term physical fate of dredged material discharged into the aquatic environment, WES is considering conducting laboratory and field experiments. Initially, laboratory tests would be conducted to relate various empirical model coefficients (e.g., entrainment, drag, friction, settling, and apparent mass) to disposal material properties and to gain an increased understanding of the physical processes that occur during the open-water disposal of dredged material. Based on the success of these experiments and subsequent numerical model enhancements/modifications, field verification experiments may be conducted.

General Approach

4. This report addresses the feasibility of performing laboratory experiments to aid in the modification and enhancement of existing numerical models for predicting the physical fate of dredged material discharged into open water. The first major section of this report focuses on the investigation of scaling laws to determine the feasibility of accurately simulating prototype dredged material disposal behavior for various cohesive and noncohesive sediments, and to provide input to the physical sizing of the laboratory facility. The second major section discusses the general design requirements for the facility, including the types of equipment and measurement techniques required to monitor rates of cloud entrainment, rates of spreading on the bottom, disposal material properties, suspended sediment concentrations, velocity distributions, and other key parameters of interest. Typical testing scenarios for various discharge conditions are included in this discussion.

PART II: INVESTIGATION OF SCALING LAWS

Dredged Material Disposal Methods

5. A variety of methods are available for the disposal of dredged material in estuarine and coastal marine environments, including instantaneous, continuous, and mixed (i.e., somewhere between instantaneous and continuous). These methods are first briefly described. The descriptions are then followed by explanations of the physical processes that evidently occur. The remainder of this chapter consists of individual sections explaining the scaling analysis for each type of discharge method.

6. Much of the material dredged in the United States is presently discharged by either bottom dump barges or hopper dredges. These vessels usually are partitioned into compartments, each having a set of hinged bottom doors that open downward. The compartments are opened sequentially. The time required to discharge each compartment is commonly a fraction of a minute, although the time to discharge all of the compartments is roughly the number of compartments times 1 min per compartment (Tetra Tech 1982). An increasingly popular method of disposal is by the use of split-hull or clamshell barges. The split-hull barge is opened by gradually widening the two halves of the barge hydraulically. Depending on the width of the opening, the barge can discharge material in as little as a few seconds to much longer times if desired. The material discharged from these barges commonly has a water content not appreciably different from in situ sediments, although in some instances water is mixed with the dredged material prior to discharge in an attempt to break up cohesive silt-clay mixtures. Another method of disposing of dredged material is by continuous discharge from an open pipe, commonly from a barge. This material usually is hydraulically dredged, using a cutterhead dredge for instance, and therefore contains a higher percentage of water than in situ material.

Numerical Disposal Models

7. The physical processes that occur in the discharge of dredged material have been investigated, and some of the knowledge gained has been incorporated into numerical models. The processes are commonly divided into

three phases: convective descent, dynamic collapse, and passive transport-diffusion. During convective descent, which begins immediately on discharge, the descent of the discharge is caused by its negative buoyancy and discharge conditions. As the discharge descends, it entrains seawater, and as a result the bulk density of the discharge mixture decreases. If the water depth is sufficiently large and the seawater density stratification is sufficiently strong, then the bulk density of the discharge may equal the density of the seawater at a depth called the neutral density depth. If this occurs, then the discharge tends to stabilize near this depth and collapse. If the water depth is not great enough, the discharge mixture will impact the seafloor and form a bottom surge. The collapse of the discharge mixture either in the water column or on the seafloor is termed the dynamic collapse phase. This phase ends when the momentum of the discharge is spent. Thereafter, i.e., during the passive transport-diffusion phase, the motions of material remaining in the water column are caused by processes independent of the method of discharge. Processes occurring during this phase are not discussed further.

8. The division of these processes originates from the modeling efforts of Koh and Chang (1973) and Brandsma and Divoky (1976). In the first effort intended to model the behavior of ocean discharges, three computer programs were written, one for instantaneous discharges, another for continuous discharges from a submerged pipe, and the third for discharge into the wake of a moving barge. The first two of these models were substantially altered by Brandsma and Divoky (1976) for use in estuaries. Unsteady currents in the horizontal plane (in at most two layers) were allowed. Also, the methods of calculation for passive transport-diffusion were rewritten based on an adaptation of methods of Fischer (1972). Other models and procedures for computing one or more of the phases have been written. Johnson, Holliday, and Thomas (1978) review model development through the mid-1970's. The Brandsma-Divoky models have since become "standard." Versions of these models are presently actively supported by WES (Johnson in preparation). The discharge in the wake of a moving barge was extensively modified by Brandsma and Wu* for EXXON and is now supported actively by Brandsma as the Mud Discharge Model for predicting the fate of drilling fluids discharged into the marine environment

---

* M. G. Brandsma and F. Wu. 1980. "Development of Model to Predict Drilling Mud Plume Concentrations in Offshore Operations," draft final report, Pasadena, CA.

(Brandsma, Ayers, and Sauer 1983). Neither the Brandsma and Wu nor the Brandsma, Ayers, and Sauer models is commonly used for determination of the fate of discharged dredged material; therefore, neither is discussed.

9. The computations in the convective descent phase of the Brandsma and Divoky models are based on conservation of momentum, relative buoyancy, and liquid and solid volumes. Entrainment, drag, and possible particle settling out of the discharge are also considered. Each of these depends on one or more dimensionless constants, which must be specified. Similar conservation laws are used for predicting the behavior of the discharge cloud formed by an instantaneous discharge or for the jet formed by a continuous discharge from a submerged pipe. In addition, constants must be specified for the density gradient inside the discharge at commencement of dynamic collapse, and for the friction between the seafloor and the discharge. Accurate predictions from the models depend on proper knowledge of the coefficients, assuming that the formulations of the physical processes used in the model are adequate. If the formulations are not sufficiently detailed, however, then determination of the coefficients based on extensive experiments is not likely to produce accurate model estimates.

Dredged Material Disposal Characteristics

10. The characteristics of dredged material vary substantially. The material ranges from gravel to clays with particle size distributions depending on the site. The sediment particle densities usually range from 2.6 to 2.7 g/cm^3. In situ bulk densities commonly range from 1.4 to 1.7 g/cm^3 or more. Clamshell dredging tends not to disturb the in situ properties (i.e., the degree of compaction and clumping of clay-silt mixtures) of the dredged material. In contrast, hydraulic dredging tends to destroy the in situ properties of the material and mixes the sediments with water, the addition of which lowers the bulk density of the water-sediment mixture (compared to its in situ value). In lieu of site-specific information, the voids ratio of both dredged material particles and bulk material is commonly assumed to be 0.8. The particle fall velocities of sand and gravel particles are normally computed using Stokes' law based on particle density and diameter. Clay and silt particles are usually cohesive, and thus their particle fall velocities are usually a function of sediment concentration. Commonly, fall velocities for

dilute clay-silt mixtures are dependent on the concentration raised to a power, usually 4/3. If the particles are bound together in clumps, then the fall velocity of the clump is calculable as a noncohesive particle.

11. Discharge of dredged materials is usually into estuarine waters or on the continental shelf. Occasionally, material is discharged off the shelf; however, this practice is not used in many locations due to excessive transportation costs. Dredged material discharges usually occur in water depths of less than 700 ft,* with continuous discharges usually in relatively shallow water. The volume of dredged material discharged from barges and/or hopper dredges ranges approximately from 500 to 4,000 yd^3. The speed of the barge during discharge operations usually does not exceed 4.0 knots.

Model Scaling Analysis

Convective descent phase

12. In the following discussion a dimensional analysis is presented for a stationary or moving barge that discharges material instantaneously or over a relatively short time period. The discussion concludes with a brief description of the modifications required to model a continuous discharge from a submerged pipe. The basic formulation used in both of the models DIFID and DMFJ for the convective descent phase is very similar to those presently accepted (Turner 1986) when the discharge is stationary, is into a quiescent environment, and contains no solids. The formulations in Turner (1986) will be used to begin the analysis. The analysis will then consider the effects of barge speed, current speed, and release time (in the case of an "instantaneous" discharge) on the results. Some effects of individual particle size will also be considered, but during convective descent the behavior of the discharge is commonly thought to be governed by the bulk, and not the constituent, properties of the discharged material. Processes that occur during dynamic collapse are not as well understood as processes that occur during convective descent. The formulations currently in the models are used as a start, and are supplemented with additional results. Treatment by both models of sediment transport processes that occur during dynamic collapse on the bottom is simple. Advances in understanding of sedimentary processes and the

---

* A table of factors for converting non-SI units of measurement to SI (metric) units is found on page 3.

motion of gravity currents during the past decade are used to modify the treatment in the models.

13. The dimensional analysis procedure used in this section employs the Buckingham pi theorem (Fischer et al. 1979). This theorem states that given variables representing physical quantities* q_1, $q_2 \ldots q_n$ ($q_2 \ldots q_n$ assumed independent) with k different physical dimensions, and $q_1 = f(q_2 \ldots q_n)$, then there are $n - k$ dimensionless groups $\pi_1 \ldots \pi_{n-k}$ with $\pi_1 = f(\pi_2 \ldots \pi_{n-k})$. This theorem is usually applied by first determining the dimensionless groups of initial conditions. Independent parameters to be calculated are nondimensionalized and then set to undetermined functions of the dimensionless groups of initial conditions. The algebraic manipulations required to obtain the dimensionless parameters are not provided herein. In the following, the mass, length, and time dimensions are M, L, and T, respectively. In a model, physical and dimensionless parameters are distinguished from prototype parameters by the subscript m. Model length and time scales are denoted L_R and T_R, respectively. Ideal similitude between a model and the prototype occurs when all of the dimensionless parameters of importance are the same in both the model and the prototype.

14. In the following analysis, only undistorted models (i.e., models in which the horizontal and vertical scales are identical) are considered. Distorted models for coastal and hydraulic engineering problems are often used. However, as summarized by Graf (1971), distorted models have disadvantages, among which are that "velocities are not necessarily correctly reproduced in magnitude and direction," and that "there is an unfavorable psychological effect on the observer who views distorted models." Until the dynamics of phenomena produced in undistorted models are well understood, it is the authors' opinion that distorted models should not be used.

15. In the following discussions, the x-axis defines the horizontal direction parallel to the motion of the barge (assumed to be travelling at a constant speed and direction during discharge operations), the y-axis defines the horizontal direction perpendicular to the x-axis, and the z-axis is in the vertical direction with value increasing with increasing depth and having the value zero at the sea surface. The following variables are used:

$\rho_a(z)$ = receiving water density where z is depth

---

* For convenience, symbols are listed and defined in the Notation (Appendix A).

u_B = speed of the barge

u = current velocity

ν = kinematic viscosity of seawater

g = acceleration due to gravity

At the time of the release, the following variables are used:

b_0 = radius of the discharge cloud

w_0 = fall velocity of the cloud

ρ_0 = bulk density

At time t after release, these same quantities are b, w, and ρ, respectively. A total of J solid particle types, in addition to cohesive clay, are assumed to be discharged. The fall velocity of each particle type is w_j (j=1...J) and the particle velocity of cohesive clay is assumed to be solely a function of volume concentration C.

16. In the convective descent phase, the motion of the descending discharge cloud is assumed to be primarily dependent on bulk parameters, and only weakly on individual particle types. The nine initial parameters of importance are as follows:

Parameter	Dimension
b_0	L
w_0	L/T
ρ_0	M/L^3
u_B	L/T
u	L/T
$\rho_a(0)$	M/L^3
g	L/T^2
N (Brunt-Vaisala frequency, or buoyancy)	L/T
ν	L^2/T

By the Buckingham pi theorem, there are six (i.e., 9 - 3) dimensionless parameters. These parameters are chosen to be:

$$\frac{g'b_0}{w_0^2}\ ,\ \frac{\rho_a(0)}{\rho_0}\ ,\ \frac{b_0w_0}{\nu}\ ,\ \frac{N^2b_0}{g}\ ,\ \frac{u_B}{w_0}\ ,\ \frac{u}{w_0}$$

(labeled $\pi_1 \ldots \pi_6$, respectively) where

$$g' = g \frac{\rho_0 - \rho_a(0)}{\rho_1} \tag{1}$$

in which ρ_1 is a reference density in the environment, and

$$N^2 = \frac{g \left[\frac{d\rho_a(z)}{dz}\right]}{\rho_1} \tag{2}$$

The independent parameters to be predicted are b , w , and t (time). In dimensionless terms,

$$\frac{b}{b_0} = f_1 \tag{3}$$

$$\frac{w}{w_0} = f_2 \tag{4}$$

$$\frac{t^2 g'}{b_0} = f_3 \tag{5}$$

where f_1 , f_2 , f_3 are functions of the six dimensionless constants $\pi_1 \ldots \pi_6$. These three functions are also weak functions of the dimensionless particle fall velocities w_j/w_0 .

17. Suppose a model having length scale L_R is used. Then the six dimensionless parameters $\pi_1 \ldots \pi_6$ as well as the three independent dimensionless parameters b/b_0 , w/w_0 , and $t^2 g'/b_0$ must be the same in the prototype as well as the model. The length scale L_R is used to scale all lengths, for example $b_m = L_R b$. The time scale T_R , i.e., $t_m = T_R t$, is determined by the relations:

$$\frac{g' b_0}{w_0^2} = \frac{g'_m b_{0m}}{w_{0m}^2} = \frac{T_R^2 g'_m b_0}{L_R w_0^2}$$

which implies that $T_R^2 = L_R g'/g'_m$. Thus $w_m = L_R w/T_R$. The receiving water density profile must be geometrically similar to that in the model, i.e., $\rho_a(z)/\rho_{am}(T_R z)$ must be constant for all z . In addition, the requirement that

$$\frac{N^2 b_0}{g} = \frac{g\left[\frac{d\rho_a(z)}{dz}\right]}{g\rho_a(0)} = \frac{g\left[\frac{d\rho_{am}(z_m)}{dz_m}\right]}{g\rho_{am}(0)} = \frac{N_m^2 b_{0m}}{g} \tag{7}$$

is equivalent to the condition that

$$\frac{d\rho_{am}(z_m)}{dz_m} = \frac{d\rho_a(z)}{dz}\,\frac{\rho_{am}(0)}{\rho_a(0)}\,\frac{1}{L_R} \tag{8}$$

Also, $\rho_{am}(0)/\rho_{0m}$ must be equal to $\rho_a(0)/\rho_0$.

18. The final requirement for similitude is that the flow Reynolds number $Re = b_0 w_0/\nu = b_{0m} w_{0m}/\nu_m = Re_m$. Because salt water will be used in the model, ν_m is approximately ν and differs from ν only because of temperature and salinity variations between the ocean and the model. In the ocean, ν is on the order of 10^{-5} ft^2/sec (i.e., 10^{-6} m^2/sec). For b and w scaled by L_R and L_R/T_R , respectively, Re_m is approximately a factor of L_R^2/T_R too small. For a hemispherical 500 yd^3 discharged in 10 sec from a barge, $b_0 = 19$ ft and $w_0 = 1.9$ sec (employing the estimate that the release time is approximately b_0/w_0). Assuming that $\nu = 1.2 \times 10^{-5}$ ft^2/sec (as would be the case if the water temperature were 20° C and the salinity were 34 ppt (Fischer et al. 1979)), $Re = 3.0 \times 10^6$. In a model having the same ν , a length scale L_R of 1/100, and a time scale T_R of 1/10, $Re_m = 3.0 \times 10^3$. If the descending discharge cloud behaves as a solid sphere, then this inequality may not be serious, in that the drag coefficient C_D is roughly constant (within a factor of two (Schlichting 1968)). By default, the model DIFID assumes that the drag coefficient is a constant having the value 0.5. Limited experimental evidence by Bowers and Goldenblatt (1978) when compared to predictions made by DMF (an earlier version of DIFID) required somewhat lower values of the drag coefficient. With the exception of Reynolds number, complete similitude can be achieved in a reasonably scaled experiment.

Therefore, the behavior of the drag coefficient in model experiments is of interest.

19. Several comments should be made. Experience with the model DIFID suggests that the behavior of the descending discharge cloud is essentially insensitive to reasonable variations in the receiving water density profile near (on the order of several hundreds of feet) the sea surface. Therefore, geometric similitude of the prototype and model density profiles is probably not necessary until the water depths are great enough so that dynamic collapse may occur. If the descending cloud is near dynamic collapse, then predictions of the motions of the cloud may become very sensitive to the drag coefficient, which steadily increases for values of Reynolds number less than 10^3 (for a solid sphere, refer to Figure 1). In many situations, the water depths are

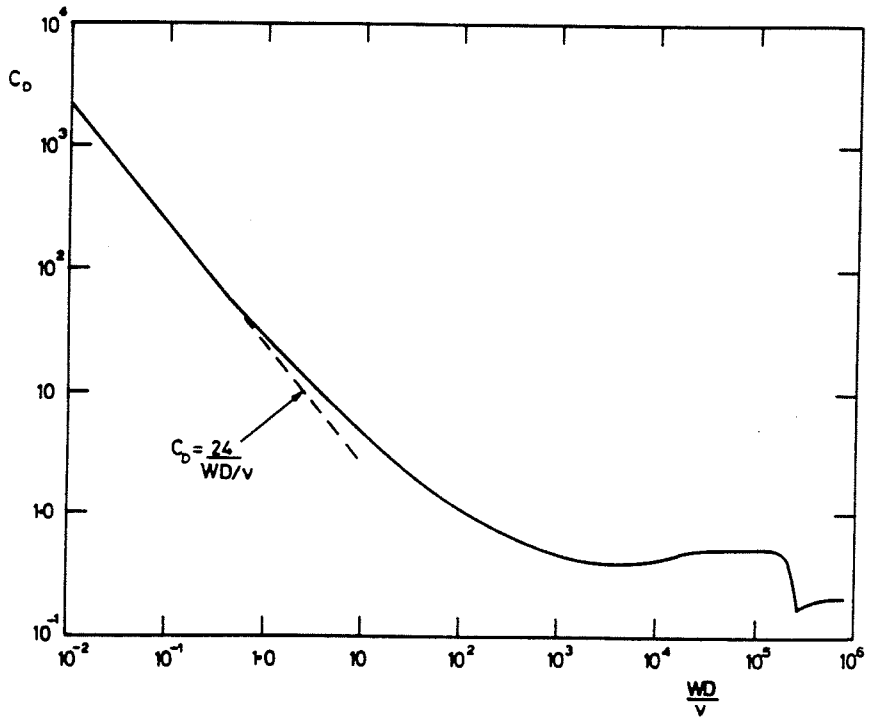

Figure 1. Variation of drag coefficient with Reynolds number for a sphere falling in an infinite fluid

relatively shallow and dynamic collapse in the water column is not expected. However, off the continental shelf, water depths increase rapidly and the receiving water density gradients in the deeper layers, although weak compared to near-surface gradients, may be sufficiently high to cause dynamic collapse in the water column. As it is of some interest to determine whether this can be modeled in a tank of reasonable scale, the following simplified analysis

based on buoyant thermal physics (Turner 1986) is provided.

20. The motion of buoyant thermals in the atmosphere has been investigated for a number of years beginning with the work of Taylor during World War II (Turner 1986). The conservation equations of mass, momentum, and buoyancy for a negatively buoyant spherical "thermal" (adapted from Turner (1986) are:

$$\frac{db^3}{dt} = 3ab^2w \tag{9}$$

$$\frac{d(b^3w)}{dt} = \frac{2}{3} b^3 g' \tag{10}$$

$$\frac{d(b^3g')}{dt} = -b^3wN^2 \tag{11}$$

where a is the entrainment coefficient, which is on the order of 0.2 (for buoyant thermals). Assuming that the receiving water is linearly stratified, and therefore N is a constant, an analytical solution for b, w, and ρ using these three equations can be obtained. (This can be accomplished by differentiating Equation 10 by t and inserting Equation 11 on the right side. As a result, a second-order differential equation for b^3w is obtained which can be easily solved by standard techniques. Equation 9 can then be solved for b, and Equation 10 can be solved for ρ.) If the receiving water is unstratified, in which case $N = 0$, the solutions are:

$$b = b_0 \left[1 + \frac{4a}{b_0 \left(\frac{g_0' t^2}{3} + w_0 t \right)} \right]^{1/4} \tag{12}$$

$$w = \frac{\left(\frac{2g_0' t}{3} + w_0 \right)}{\left[1 + \frac{4a}{b_0 \left(\frac{g_0' t^2}{3} + w_0 t \right)} \right]^{3/4}} \tag{13}$$

$$\rho = \rho_a(0) + \frac{\rho_1 (g_0' b_0^3)}{g b^3} \tag{14}$$

If the receiving water is linearly stratified with $N \neq 0$, then the solutions are:

$$b = b_0 \left\{ 1 + \frac{4a}{b_0^4 f} \left[B - B \cos (ft) + A \sin (ft) \right] \right\}^{1/4} \tag{15}$$

$$w = \frac{A \cos (ft) + B \sin (ft)}{b^3} \tag{16}$$

$$\rho = \rho a(0) + \rho 1 \left\{ \frac{\frac{-N^2 \left[A \sin (ft) - B \cos (ft) + B \right]}{f} + b_0^3 g_0'}{b^3 g} \right\} \tag{17}$$

where

$$f = (2/3)^{1/2} N \tag{18}$$

$$A = b_0^3 w_0 \tag{19}$$

$$B = (2/3) b_0^3 \frac{g_0'}{f} \tag{20}$$

The depth at which dynamic collapse occurs is estimated as the depth at which the cloud density $\rho(t)$ is identical to the receiving water density $\rho_a[z(t)]$. The equation for the cloud density can be written as a function of b (instead of t) as:

$$\rho = \rho_a(0) + \rho_1 \left[\frac{\frac{-N^2 (b^4 - b_0^4)}{4a} + b_0^3 g_0'}{g b^3} \right] \tag{21}$$

Using Equation 22

$$z = \frac{b(t)}{a} \tag{22}$$

this equation can be written as a function of z as:

$$\rho = \rho_a(0) + \rho_1 \left[\frac{\frac{-N^2(z^4 - z_0^4)}{4} + z_0^3 g_0'}{gz^3} \right] \tag{23}$$

The receiving water density can be written as

$$\rho_a(z) = \rho_a(0) + \frac{\rho_1 N^2 z}{g} \tag{24}$$

The depth at which the cloud density is the same as the receiving water density is obtained solving the equality $\rho(z) = \rho_a(z)$ for z. The depth z satisfying this equality is

$$z = z_0 \, 0.8^{1/4} \left[1 + \frac{g_0'}{N^2 z_0} \right]^{1/4} \tag{25}$$

In the ocean, a strong receiving water density gradient might be on the order of 1 sigma-t unit per 100 m while a weak gradient might be on the order of 0.1 sigma-t unit per 100 m. These gradients correspond to values of N^2 of approximately $10^{-4}/\text{sec}^2$ and $10^{-5}/\text{sec}^2$, respectively. If sand were used in the model, so that $g_0' = 16.2$ m/sec^2, then z would be approximately 196 m and 349 m, respectively, assuming that the discharge volume is 500 yd^3 and that a is 0.2. If lighter model material (such as glass) is used, then even smaller values of z can be obtained. These computations suggest that dynamic collapse in the water column can be modeled when the receiving water is weakly stratified if light sediment particles are employed.

21. The dimensional analysis of convective descent also indicates that

the ratio of the particle fall velocity to the initial cloud velocity w_j/w_0 should be the same in the model as in the prototype. Therefore the model fall velocity w_{jm} should equal $L_R w_j/T_R$ for both noncohesive and cohesive particles. The particle fall velocity for a spherical noncohesive particle having grain diameter D is

$$W^2 = \frac{g(\rho_s - \rho)}{\rho} \frac{4}{3} \frac{D}{C_D} \tag{26}$$

where

ρ_s = particle density

C_D = drag coefficient which is a function of Re (i.e., WD/ν)

The behavior of the drag coefficient as a function of Reynolds number is shown in Figure 1. In the Stokes range (i.e., WD/ν less than 0.1, here assumed to be unity with only a slight error as shown in Figure 1),

$$C_D = \frac{24}{\left[\frac{WD}{\nu}\right]} \tag{27}$$

In this case, the particle fall velocity is

$$W = \frac{gD^2}{18\nu} \frac{(\rho_s - \rho)}{\rho} \tag{28}$$

In both the prototype and the model, ν is on the order of 10^{-6} m^2/sec. Thus for quartz particles having a density of approximately 2.65 g/cm^3, the particle Reynolds number is less than 1.0 for values of D less than 100 μm (1 μm = 1 micron). If both prototype and model particle diameters have particle Reynolds numbers less than 1.0, then the model particle diameter should be chosen to satisfy

$$D_m^2 = \frac{\left[\frac{(\rho_s - \rho)}{\rho}\right]}{\left[\frac{(\rho_s - \rho)}{\rho_m}\right]} \frac{\nu_m}{\nu} \frac{D^2 L_R}{T_R} \tag{29}$$

From this equation it is evident that, for model particles having the same density as prototype particles, the ratio D_m/D is $(L_R)^{1/4}$. If either the prototype or the model particle Reynolds number is greater than 1.0, then the particle fall velocity must be computed using Figure 1 with the model particle diameter satisfying the equation

$$D_m = \frac{\left[\frac{(\rho_s - \rho)}{\rho_m}\right]}{\left[\frac{(\rho_s - \rho)}{\rho}\right]} \frac{C_D\left[\frac{W_m D_m}{\nu_m^2}\right]}{C_D\left[\frac{WD}{\nu}\right]} \frac{L_R}{T_R^2} D \tag{30}$$

22. Experiments and theory (Graf 1971) have indicated that particle fall velocities are dependent on particle shape and also on concentration. If nonspherical particles are used, then corrections to these formulas can be obtained. As long as the total volume of particles (V_{jm}) of each grain diameter is scaled properly (i.e., $V_{jm} = L_R^3 V_j$), then concentration-dependent effects should be roughly the same in the model as in the prototype, with the difference dependent on particle Reynolds number effects discussed briefly by Sleath (1984).

23. Invariance of the ratio w_j/w_0 for cohesive particles must also be attained. Cohesive particles in the form of clumps in the prototype must be assumed to behave as noncohesive particles that do not break up during either convective descent or dynamic collapse. In this case, the scaling for noncohesive particles should be used. The particle fall velocity of cohesive particles is complex. In many cases, the fall velocity is concentration dependent and may be described as:

$$w_c = \beta C^n \tag{31}$$

(where β is a constant) for concentrations not so large that hindered settling occurs. The exponent n in Equation 31 is roughly 4/3 for some materials (Dyer 1986). Several modeling schemes are possible assuming that this rule is approximately valid. The first assumes that the type of the cohesive material to be modeled can be chemically altered (or otherwise changed) so that n is the same for both model and prototype cohesive

particles and that the constant β_m satisfies the relation:

$$\beta_m = \frac{L_R}{T_R} \beta \tag{32}$$

Another possibility is to use the same material in both the model and prototype, but model the cohesive particle concentration using:

$$C_m = \left[\frac{L_R}{T_R}\right]^{1/n} C \tag{33}$$

This can be accomplished by using a smaller volume of clay in the model than required by length scaling alone. To ensure that the cloud has the correct bulk density, alteration of the volumes of noncohesive particles may be required. If so, then the concentration-dependent fall velocity effects mentioned previously will introduce additional complications to the interpretation of the model results. In view of the variety of clays and clay-silt mixtures found in coastal and estuarine marine sediments, the fall velocity as a function of concentration (and other dynamic parameters as required) of the material used in the model should be experimentally determined and used to develop the proper scaling rule.

24. The requirements described in the preceding discussions for noncohesive and cohesive sediments are probably not strictly necessary for an adequate description of the bulk behavior during convective descent if the descending cloud is not decelerating when it impacts the seafloor. The particle diameter results are required if the descending cloud is significantly decelerating (in which case individual particles may begin to fall out of the cloud), or if estimates of the amount of sediment left behind in the water column in the wake of the descending cloud are desired.

Dynamic collapse phase

25. The scaling rules for dynamic collapse in the water column are the same as provided for convective descent, with the particle diameter rules being required. During the beginning of this phase, the descending cloud will begin to flatten. When this occurs, the drag coefficient as a function of Reynolds number curve shown in Figure 1 for spheres will no longer be valid.

26. Technically, apart from the choice of bottom sediment type, no

scaling arguments are needed to determine the scaling required to investigate dynamic collapse on the seafloor. However, the behavior of sediment particles in the surge created by dynamic collapse on the bottom requires different considerations than in the water column. In view of this, scaling arguments are provided assuming that the characteristics of the descending cloud are known. In the following discussions, it is assumed that the discharge cloud is descending vertically when it impacts the seafloor. At this instant, the cloud is assumed to have diameter d_I and velocity w_I, to have entrained $S_a - 1$ times its original volume of receiving water into the cloud (S_a is the volume of receiving water entrained during convective descent), and to have bulk density ρ_I. The time required for the cloud to completely impact the seafloor is t_I. All of these parameters can be measured in a properly scaled convective descent experiment. The mean bottom sediment diameter is labeled D_b. For convenience, it is assumed that on impact the cloud is cylindrical and that the cylindrical cloud spreads radially on the bottom. The initial radius, height, and radial speed of the bottom cloud are assumed to be $r_0(0.5d_I)$, h_0, and U_0, respectively. Conservation of volume flux then requires that $U_0 = w_I d_I^2/(8r_0h_0)$. The initial parameters of importance are as follows:

Parameter	Dimension
t_I	T
g	L/T^2
r_0	L
h_0	L
U_0	L/T
ρ_I	M/L^3
$\rho_a(d)$	M/L^3
D_b	L
ν	L^2/T

By the Buckingham pi theorem, there are six (i.e., 9 - 3) dimensionless parameters. These are chosen to be:

$$\frac{U_0^2}{g_I' h_0}, \frac{U_0 D_b}{\nu}, \frac{U_0 h_0}{\nu}, \frac{t_I U_0}{r_0}, \frac{t_I U_0 h_0}{r_0^2}, \frac{\rho_I}{\rho_a(d)},$$

where $g_I' = [\rho_I - \rho_a(d)]/\rho_I$ and d is the water depth. The first three of

these are the Richardson number, the bottom sediment Reynolds number, and the flow Reynolds number, respectively. The fourth parameter is a dimensionless release time and is a measure of whether the time duration of the bottom surge is short (i.e., if $t_I U_0/r_0 \ll 1$) or long (i.e., if $t_I U_0/r_0 \gg 1$). The latter occurs for continuous discharges, but may or may not occur for a barge discharge. The fifth parameter is a normalized total volume.

27. Suppose a model having length scale L_R and time scale T_R is used. Invariance of the Richardson numbers of the prototype and the model requires that:

$$\frac{U_0}{g'_I h_0} = \frac{U_{0m}^2}{g'_{Im} h_{0m}} = \frac{L_R}{T_R^2 g'_{Im}} \tag{34}$$

which implies that $T_R^2 = L_R g'_I / g'_{Im}$. The factors L_R and T_R can be used to scale lengths and times not related to sediment particles.

28. The radial speed of the bottom surge is dependent on the entrainment rate of fluid through the top of the surge, the frictional losses due to interaction of the surge with the seafloor, and (to a lesser extent) the behavior of sediment particles suspended within the cloud. At the termination of dynamic collapse (i.e., when the radial velocity of the surge vanishes), the distribution of suspended solids within the cloud must be measured for use as initial conditions for the passive diffusion phase. The rate of entrainment of receiving water fluid into the cloud at a given radius R is dependent on the Richardson number $U^2(R)/g'_I h(R)$. If the model and prototype flows are in similitude, then the Richardson number should be invariant (as long as both flows are turbulent). The effect of friction will be the same in the model as in the prototype if the shear velocity in the model u_{*m} is L_R/T_R times the shear velocity u_* in the prototype.

29. The calculation of shear velocity for a turbulent uniform flow over a seafloor can be accomplished by well-known methods (Dyer 1986). Such a flow is considered to consist of a logarithmic layer beginning at a height of Z_0 (the bed roughness height) above the bed. At a height of about $1{,}000\nu/u_*$, an outer layer (sometimes called the velocity defect layer) begins. Similarity between model and prototype requires that the roughness Reynolds number $u_* k_s/\nu$ (where k_s is the bed roughness) be the same in both the model and

the prototype so that the ratio of Z_0/k_s is invariant. The bed roughness is a constant (on the order of 1.0) times the bed particle diameter. Thus equality of the roughness Reynolds numbers is the same as the equality of the bottom sediment Reynolds number, i.e.,

$$\frac{u_* D_b}{\nu} = \frac{u_{*m} D_{bm}}{\nu_m} = \frac{L_R u_* D_{bm}}{T_R \nu_m} \tag{35}$$

This equality is satisfied for $D_{bm} = (\nu_m/\nu)(T_R/L_R)D_b$.

30. The bed particle density in the model is not important unless the speed of the bottom surge is high enough to cause erosion in the prototype. The critical shear stress needed to erode sediments in a steady flow is shown on the Shields diagram in Figure 2. Similitude of critical shear stresses in the model and prototype requires that

$$\frac{\rho_a(d)u_*^2}{[\rho_b - \rho_a(d)]gD_b} = \frac{\rho_{am}(d)u_{*m}^2}{[\rho_{bm} - \rho_{am}(d_m)]gD_{bm}} = \frac{\rho_{am}(d)L_R^2 u_*^2}{[\rho_{bm} - \rho_{am}(d_m)]T_R^2 gD_{bm}} \tag{36}$$

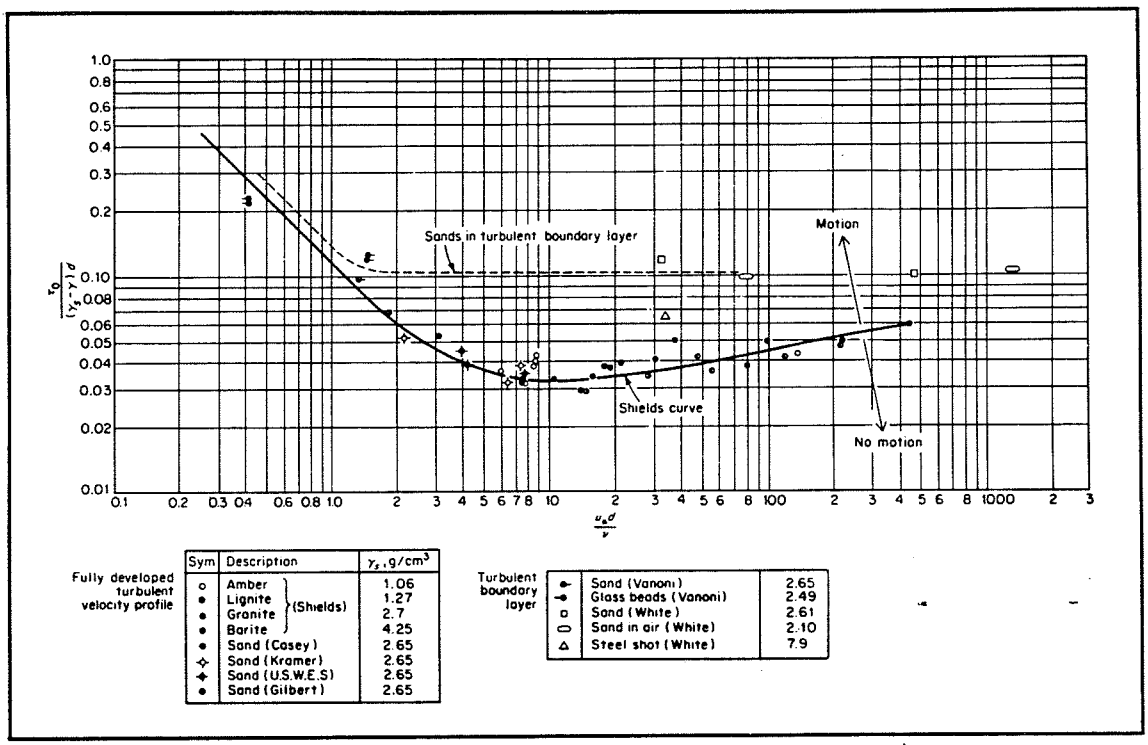

Figure 2. Shields diagram of dimensionless critical shear stress versus shear Reynolds number

where ρ_b is the bed particle density. Using the result for D_{bm} in this relation, then

$$\rho_{bm} = \rho_{am}(d_m) \left[1 + \frac{\rho_b - \rho_a(d)}{\rho_a(d)} \frac{L_R^3}{T_R^3} \frac{\nu}{\nu_m} \right] \tag{37}$$

This requires the bed sediment particles in the model to be very light. Even if this is accomplished, erosion of bed sediments in the model will probably not be in similitude because most total load formulas (Sleath 1984) contain a dependence on D_b apart from the bed sediment Reynolds number. The scale dependence of D_b in these terms should be L_R, not $(\nu_m/\nu)T_R/L_R$ as given in Equation 37.

31. The behavior of suspended discharged particles in the bottom surge is dependent on the ratio $w_j/(0.4u_*)$ (Graf 1971) since the vertical eddy diffusivity in a bottom boundary layer is approximately $0.4u_*z$ (where 0.4 is von Karman's constant). If the ratio is much less than unity, the particles will tend to remain suspended, while if the ratio is much greater than unity, the particles will tend to settle. Assuming that u_* is in similitude, and that the model particle diameters have been chosen as discussed previously (in the convective descent discussion), then the ratio $w_j/(0.4u_*)$ is in similitude. The amount of cloud particles remaining in the surge after termination of dynamic collapse, however, is not entirely produced in the model. In the prototype, cloud particles that settle may be subsequently eroded and transported. As discussed previously, the erosion rate cannot be properly modeled. In the prototype coastal and estuarine waters, some receiving water currents are almost always present. These currents cause boundary layer currents with a typical shear velocity on the order of 1.0 cm/sec. Thus particles in the prototype having a value of $w_j/(0.4u_*)$ less than unity will tend to remain suspended at the end of dynamic collapse. If the model tests are conducted in an initially quiescent tank, then the shear velocity at the end of dynamic collapse is likely to be essentially zero, and particles remaining suspended will have begun to fall according to their fall velocity alone.

Other Scaling Considerations

32. Implicit in the preceding discussions has been the assumption that

the model and prototype flows are turbulent, and remain so during most of the time required for convective descent and dynamic collapse. This assumption is valid in the prototype, but is less valid in the model. For flow Reynolds numbers on the order of 10^3 or greater, the flows are turbulent. As the flow Reynolds number decreases below this value, either due to deceleration of the descending cloud as dynamic collapse in the water column is approached or to radial spreading of the bottom surge, then whether or not the flow remains turbulent depends on the decay rate of turbulent energy. Because of this, the flow may remain turbulent below values of 10^3. Estimates of the extent of this effect could be investigated in the model. It is suggested that all model experiments be chosen so that the flow is initially turbulent, with a flow Reynolds number high enough, say, 10^4, so that the Reynolds number does not drop below the critical value.

33. The dimensional analysis presented for a barged discharge over a relatively short time period is also valid for a continuous discharge from a submerged pipe. In this case, the pipe diameter is b_0, and the velocity of the discharge is w_0, which is calculated by dividing the flow rate by the effective pipe area at the end of the pipe. In the terminology commonly used to describe buoyant plumes (Muellenhoff et al. 1985) for instance, the dimensionless parameter $g'b_0/w_0^2$ (derived earlier in the discussion of discharge from a barge) is the inverse of the square root of the port Froude number. The bulk discharged sediment parameters influence the behavior of sediment-laden jets and plumes immediately after discharge less than after a (more or less) instantaneous discharge from a barge. In a jet or a plume, the ratio b/z is approximately 0.10 assuming no particles are present in the discharge. Experiments by Ditmars and McCarthy (1975) indicate that this ratio increases as the particle content of the discharge increases.

34. The dimensional analysis described in this section is required both to determine the feasibility of accurately simulating the physical phenomena of dredged material disposal in a scaled model as well as to determine the physical sizing requirements for an appropriate test facility. A summary of the dimensional analysis is presented at the beginning of Part III of this report.

PART III: PRELIMINARY DESIGN OF TESTING FACILITY

Sizing and Layout of Facility

35. The purpose of this section is to develop recommendations on the physical dimensions and shelter requirements of the testing facility required to accommodate a range of laboratory experiments for dredged material disposal. Recommendations are presented regarding the types of laboratory monitoring equipment and monitoring strategies for conducting scaled dredged material disposal tests.

Summary of scaling law analysis

36. The dimensional analysis presented in Part II of this report indicated that scaling of the prototype is possible for both convective descent and dynamic collapse provided that the Reynolds number appropriate for each phase is high enough so that turbulent flow occurs (except during the end of dynamic collapse). Froude number similitude is always required. Flow Reynolds number similitude is never achieved in the water column, but is required (assuming that dynamic collapse occurs on the bottom) for the roughness Reynolds number applicable to the bottom sediments. This is possible by increasing the bottom sediment diameter.

37. The Reynolds number requirements put a limit on the scales that can be used. The flow Reynolds number in the model at the beginning of either the convective descent or dynamic collapse phases should be high enough to cause turbulent flow. If this number is, say, 10^4, then the prototype Reynolds number is $10^4 T_R / L_R^2$. For many discharge possibilities, the length scale factor should exceed 1/100 (i.e., $L_R \geq 1/100$). Decreasing the particle densities used in the model compared to those in the prototype is a method of enlarging the range of permissible length scales. It should be recalled that the Reynolds number arguments for convective descent for a discharge from a barge were based on experimental results for solid spheres, and not descending clouds. The Reynolds number behavior of such clouds should be investigated, and the results incorporated into the scaling analysis of Part II of this report. The decay of turbulence in decelerating flows should also be monitored to the extent possible.

Desired range of test conditions

38. The physical size of the testing facility is influenced by the

range of test conditions for anticipated experiments. The ranges of various prototype parameters for potential tests have been identified as follows:

a. Water depth: 100 to 700 ft

b. Disposal volume: 200 to 4,000 yd^3

c. Bulk density: 1.5

d. Barge speed: 0.0 to 4.0 knots

e. Ambient density gradient: 0.0 to 0.000004 g/cm^3 per foot

f. Material size classifications and settling velocities:

Classification	Settling Velocity fps
Clumps	0.50
Clay	0.0004
Silt	0.008
Fine sand	0.03
Medium sand	0.08

39. It is anticipated that initial dredged material disposal model experiments will be kept simple; that is, they will be conducted as stationary barge releases into quiescent waters having no vertical salinity gradient. Depending on the outcome of these initial tests, future investigations may involve introducing other variables such as ambient currents, a stratified water column, towed barge disposal, and continuous moving pipe discharge. Sizing of the test facility will take into account the various potential test variables.

DIFID model estimates

40. The size of the testing facility should accommodate the desired range of test conditions with the primary goal being the limitation of side-wall boundary effects on the convective descent and bottom collapse phases of the discharge event. Initial estimates of the physical dimensions of the sediment cloud size at the end of the bottom collapse phase were determined using the numerical model DIFID. For purposes of this modeling effort, disposal was assumed to occur below the water surface from a split-hull barge. This approach resulted in conservative estimates of the size of the cloud at the end of the bottom collapse phase. Six input parameters were varied for the DIFID runs: disposal volume, water depth, bulk density, barge speed, ambient density difference, and sediment size fraction. The ranges of values

for each of the input parameters is given in Table 1. A total of 1,440 DIFID model runs were made to cover all combinations of the six input parameters.

41. The DIFID model predicted maximum bottom sediment cloud diameters of 595, 1,076, 1,718, and 2,108 ft for depths of 100, 300, 500, and 700 ft, respectively, at the end of dynamic collapse. As would be expected, the maximum cloud diameters for each of the depths occurred as a result of the large 4,000-yd^3 discharge and a barge speed of 4.0 knots. A summary of the results of the DIFID model runs is given in Table 1. The column labeled "Maximum Concentration" is the maximum or "worst case" concentration of the sediment cloud as detected by DIFID at the end of the bottom collapse phase. This value may be somewhat misleading in that it is dependent on the computed height of the sediment cloud as it rests on the bottom at the end of dynamic collapse. In other words, if the computed height is small, then the bottom sediment cloud concentration will be large when, in fact, the cloud has essentially completely settled out of the water column and is now mainly bottom sediment. The computed time to the end of the dynamic collapse phase is also given in Table 1.

Available facilities at WES

42. In order to save time and money in constructing the dredged material disposal model, a survey of the existing facilities at WES was conducted to ascertain whether any were suitable for the proposed range of model test conditions. Two existing sumps at WES were identified as potential sites for the dredged material disposal testing facility. One sump was the Newbury Port Harbor sump, which has a depth of 8 ft and horizontal dimensions of 70 by 30 ft (Figure 3). The other was the Georgetown Harbor sump, which has a depth of 10 ft and is divided into four individual compartments, the largest of which is 35 by 30 ft (Figure 4).

43. The physical dimensions of both of these existing sumps are sufficient to properly model the range of test conditions discussed previously. However, the Georgetown Harbor sump may be more desirable for several reasons. First, the total volume of water required to fill the large Newbury Port sump to capacity is 125,600 gal compared with 78,500 gal for the Georgetown Harbor sump. Based on past experience at WES, filling these large sumps puts such a demand on the local water supply system that adequate pressure cannot be maintained, so the local authorities have restricted filling of these sumps to only certain offpeak demand hours. The smaller capacity of the Georgetown

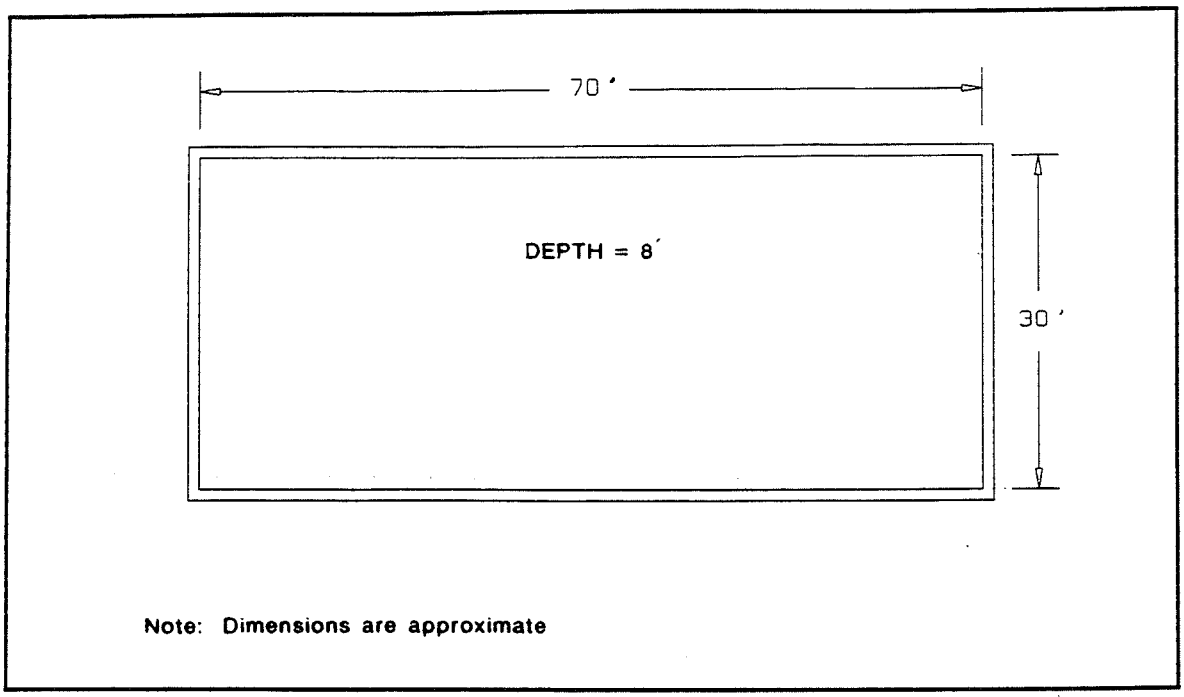

Figure 3. Dimensions of existing Newbury Port Harbor sump

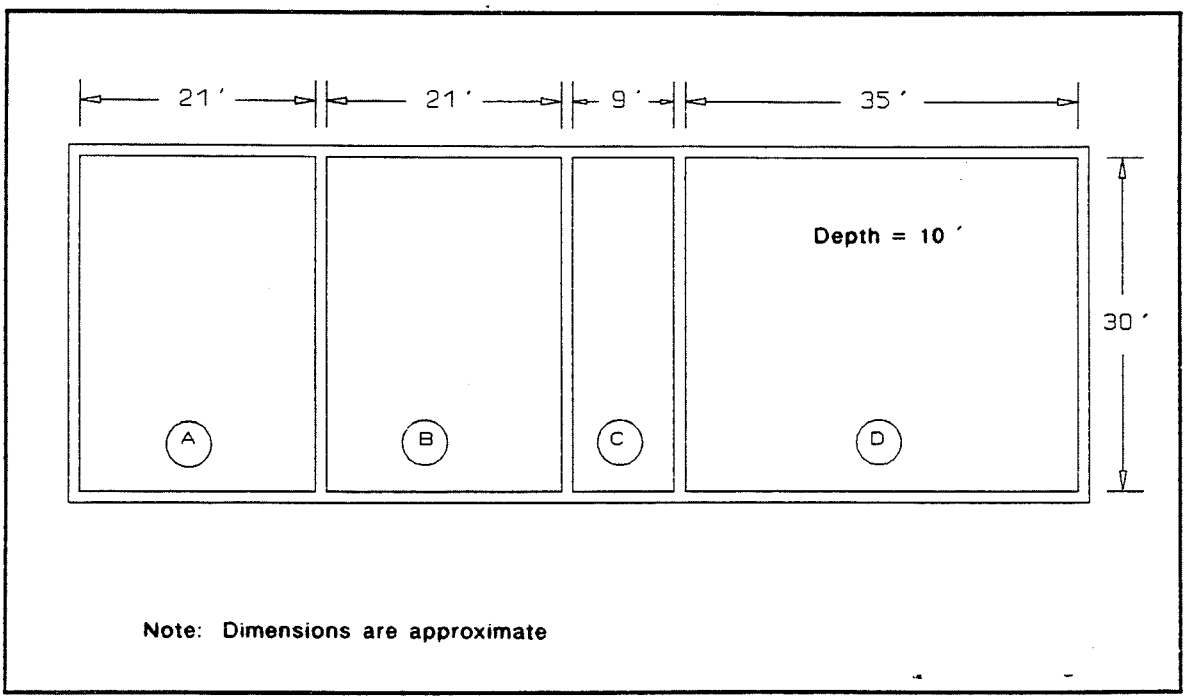

Figure 4. Dimensions of existing Georgetown Harbor sump

Harbor sump will place less demand on the local water supply and will be faster to fill. Secondly, there are two smaller compartments each measuring 21 by 30 ft in the Georgetown Harbor sump that can be used for storage of water between model tests. These two smaller compartments would eliminate the need to construct separate holding tanks, and they could also be used as mixing tanks for creating different salinities in the event a variable density test is desired. Thirdly, there is an even smaller 9- by 30-ft compartment immediately adjacent to the testing compartment that will be ideal for a viewing and filming area.

44. In addition to the sumps, other existing test equipment is also available at WES for potential use in the dredged material disposal experments. This includes, but is not limited to, microcomputers, analog-to-digital input-output interface cards, miniature electromagnetic velocity meters, conductivity-temperature sensors, turbidimeters, transmissometers, and video recorders.

Recommendations for facility layout

45. The geometric scale of the test facility is based on the DIFID model runs and the scaling laws discussed in Part II. As stated previously, it is recommended that the test facility be designed as an undistorted model; that is, the vertical and horizontal scales will be the same. For reasons listed previously, it is also recommended that the Georgetown Harbor sump be used for the test facility.

46. Depending on the type of disposal and water depth, the length scale ratio can be varied to minimize the effect of dissimilar model and prototype Reynolds numbers. The closer the model-to-prototype length scale ratio is to 1, the closer the model and prototype Reynolds numbers will be to similarity. In Table 2 various length scale ratios are shown for several different test conditions, and the resulting model depths and size of bottom sediment cloud after dynamic collapse are given based on the preliminary DIFID model runs. This table shows that with a model-to-prototype length scale ratio of 1:100, the existing Georgetown Harbor sump will accommodate all the desired test conditions except for the 4,000-yd^3 disposal towed at 4.0 knots, which requires a sump length of 37.3 ft or 2.3 ft more than is available. Using a 1:100 length scale ratio for the disposal in waters having depths of 100 ft or less may not be desirable since the model depth would be only 1.0 ft, making measurements of the convective descent and bottom collapse difficult. For the shallower

depths it would therefore be advantageous to use a larger scale such as 1:50 or 1:25. As shown in Table 2, the Georgetown Harbor sump at a 1:50 scale ratio for the 100-ft prototype depth will accommodate the quiescent dump and the 2.0-knot barge speed, but will require 38.6 ft for the 4.0-knot barge speed. At a 1:25 scale, only the quiescent disposal can be modeled in the existing Georgetown Harbor sump for the 100-ft depth case.

47. Table 2 can be used as a guide for determining whether the Georgetown Harbor sump should be altered to accommodate a broader range of test conditions. For instance, if disposal from a moving barge having a speed of 4.0 knots is considered important, then the existing 35-ft-length compartment will need to be lengthened to accommodate the bottom collapse phase of some of the test scenarios (e.g., the 4,000-yd^3 disposal at a depth of 700 ft requires a 37.3-ft-long test facility). Three alternatives are presented for implementation of the Georgetown Harbor sump as a dredged material disposal test facility. The choice of which alternative design to use will depend on available funds and the scope of the planned dredged material disposal experiments. The alternatives are given in order of increasing cost; however, no actual construction cost estimates have been made since such estimates are outside the present scope of work.

48. Alternative 1. The sump can be used basically in its existing form wherein the large 35- by 30-ft compartment (compartment D in Figure 4) will be the testing tank. The wall between compartments C and D will be altered by installing a Plexiglas viewing window measuring 10 ft high by 30 ft wide. An area adjacent to the 35-ft-length wall of compartment D will be excavated and the entire wall will be replaced with a 35- by 10-ft Plexiglas window. The newly excavated area should be at least 10 ft wide to accommodate video recording equipment and other monitoring instrumentation (Figure 5). This large window will need to be braced to support the force of water on it. However, the bracing will need to be installed so that it does not interfere with video taping and other monitoring equipment. The two solid nonviewing walls will be painted white to act as a contrasting background for filming the disposal as it falls through the water column. It would be even more ideal if a diffuse backlight system (i.e., similar to that of a drafting light table) could be fabricated along these walls to aid filming the sediment cloud descent. A temporary canopy will be constructed over compartment D to shield the testing area from sun and wind effects. It will also be necessary to install new

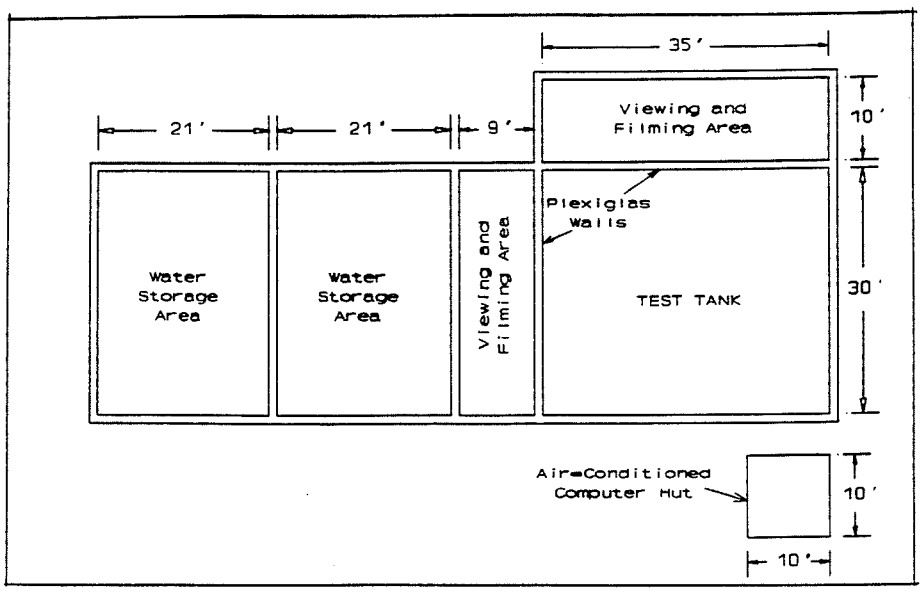

Figure 5. Georgetown Harbor sump, alternative design 1

plumbing since the present system is badly corroded from past tests using salt water. It is recommended that polyvinyl chloride plumbing be used since it will not corrode. A small air-conditioned hut measuring about 10 by 10 ft should be constructed adjacent to the test tank to house test control microcomputers and other sensitive electronic instrumentation. Appropriate electrical systems will also need to be installed in the control hut. Compartments A and B can be used for storage of water, which can be pumped to and from the main test compartment to achieve the various test depths. Compartments A and B can also be used to mix water to different salinities for possible stratified experiments.

49. Alternative 2. This scheme is similar to Alternative 1 except that the wall between compartments C and D will be completely removed to create a longer test tank having a length of 45 ft (Figure 6). This will provide a longer distance to accommodate some of the towed barge experiments listed in Table 2 that will not fit into the Alternative 1 facility. The wall between compartments B and C will be modified to provide the 10-ft-high by 30-ft-long viewing window. Under this design alternative, only compartment A will be available for storage of water, and another temporary storage tank may need to be constructed depending on the expected variation of water depths. All of the other amenities listed under Alternative 1 will also be required here.

50. Alternative 3. Again, this design is similar to Alternative 1 except that the walls between compartments C and D and compartments C and B

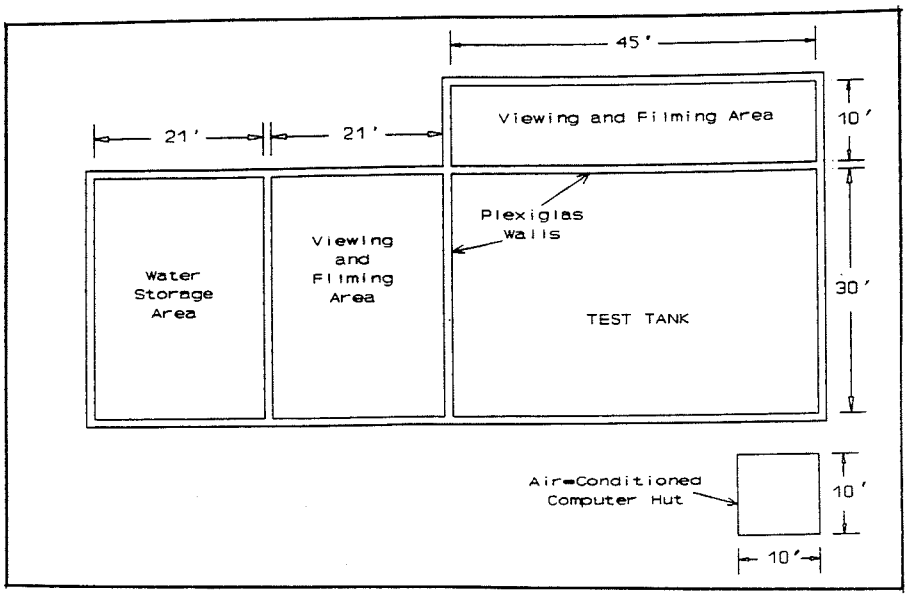

Figure 6. Georgetown Harbor sump, alternative design 2

will both be removed to provide a 67-ft-long test facility (Figure 7). The wall between compartments A and B will be altered to furnish a 10-ft-high by 30-ft-wide Plexiglas viewing window. The 67-ft wall will be replaced with Plexiglas for filming and monitoring purposes. No compartments will be available for storage of water, so temporary tanks will need to be constructed adjacent to the test facility. This design will allow nearly all the towed barge test conditions listed in Table 2 to be successfully contained within

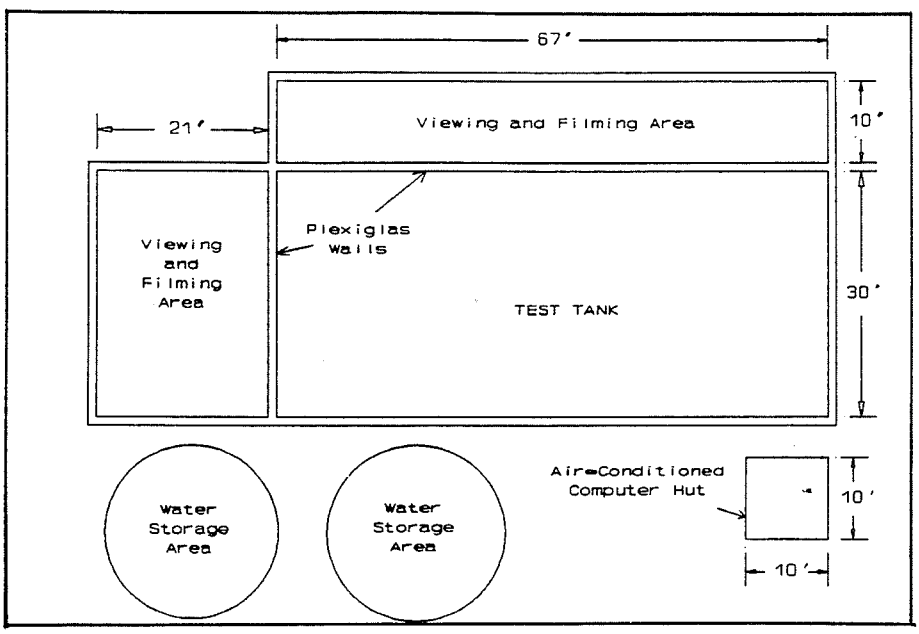

Figure 7. Georgetown Harbor sump, alternative design 3

the 67-ft length of the tank. All of the other amenities listed under Alternative 1 also will be required for this design.

51. For stationary disposal into shallow water (i.e., depths on the order of 100 ft or less), it is recommended that a model-to-prototype length scale ratio of 1:25 be used to minimize the potential effects of dissimilar Reynolds number. For towed disposals into shallow water, it will be necessary to use a length scale ratio of 1:50 to ensure that the bottom collapse phase does not encounter a sidewall. For water depths between 100 and 700 ft, Table 2 provides guidance for choosing the scale ratio.

Monitoring Techniques

52. Also of importance in designing an adequate testing facility is the development of monitoring methods and monitoring equipment to allow meaningful characterization of the complex processes governing the convective descent and bottom collapse phases of the discharge and the resultant distribution of suspended and deposited sediment.

53. The dredged material disposal experiments will involve the measurement of a number of specific properties of interest, including the size and shape of the descending cloud or discharge jet, the rate of descent of the descending cloud, the rate of entrainment of ambient water, the vertical density profile (if applicable), the vertical and horizontal currents induced by the discharge, the rate of spreading on the bottom, the suspended sediment concentration distributions, the bottom sediment accumulation distribution, and disposal material properties. A number of types of test monitoring equipment to measure these properties are described in the following paragraphs. This equipment is evaluated for applicability to the anticipated dredged material disposal model tests and its ease of use.

MVM-1 velocity meter

54. The MVM-1* is a small electromagnetic velocity meter capable of measuring the velocity of water relative to two axes simultaneously. It uses a miniature sensor that minimizes disruptions to the water environment and makes it suitable for laboratory scale model experiments. These sensors have been used successfully for making velocity measurements in a number of physical model tests, especially at the San Francisco Bay hydraulic model.

---

* A key describing the products evaluated in this study is found on page 4.

The sensors have a resolution of 0.01 fps, which translates to a model velocity of 0.05 fps assuming a model-to-prototype length scale ratio of 1:25 and a corresponding velocity scale ratio of 1:5. Since the primary direction of flow induced by the descending cloud will be vertical, one axis of the MVM-1 meters should be oriented parallel to vertical. For a towed barge, the other axis should be oriented parallel to the horizontal direction of barge movement. In the case of a stationary barge, the orientation of the second axis is not critical and can be in any convenient horizontal direction. WES presently owns three of these MVM-1 meters. To measure the velocities induced in the ambient water by the descending sediment, MVM-1 sensors should be placed at a minimum of three locations, namely, surface, middepth, and near the bottom along the center line of a stationary dump. For a towed barge, it may be necessary to obtain additional MVM-1 meters to provide adequate spatial coverage.

55. The MVM-1 can also be used to measure the velocities imparted to the ambient waters by the spreading of the sediment cloud on the bottom. For these measurements, the primary direction of movement will be horizontal and the two axes of the MVM-1 meter should be oriented parallel to the bottom plane. The standard length of cable to which the MVM-1 sensor is attached is about 6 ft. In order to reach the bottom depths for some test conditions, it may be necessary to acquire additional sensors attached to longer cables.

MCM-1 salinity meter

56. The MCM-1 is a small electronic device with a 1-in.-diam probe attached to a 6-ft-long cable. The small size of the probe minimizes disturbances to the flow field. The probe itself contains a conductivity sensor and a temperature sensor. The temperature sensor is a linearized thermistor; the instrument produces a voltage directly proportional to the water temperature in degrees centigrade. The conductivity sensor consists of two electrodes excited by a constant A-C voltage. The water between the electrodes acts as a current path whose resistance varies with the conductivity of the water. The sensor's output voltage changes linearly with changes in water conductivity. An algorithm developed under contract for the US Army Engineer District, San Francisco*, can be employed to convert conductivity and temperature data

---

* M. R. Morton. 1983. "Development of Conductivity-Temperature-Salinity Conversion Algorithm for Montedoro-Whitney MCM-1 Probes," Tetra Tech Memorandum dated 15 June 1983 (unpublished), Tetra Tech, Arlington, VA.

into sodium chloride salinity in parts per thousand (mg/ℓ). If tests calling for stratified ambient conditions are anticipated, then measurement of the salinity gradient in the test tank can be accomplished using the MCM-1 (or similar) meters. At least three of these type meters should be installed, one near the surface, one at middepth, and one near the bottom to define the density gradient due to salinity. More sample locations may be necessary to adequately describe the salinity gradient. Salinity profiling by moving an MCM-1 probe up and down vertically through the water column may be feasible, in which case a detailed description of the salinity gradient will be possible. Alternatively, discrete samples can be collected from a number of depths (perhaps 10) throughout the water column and analyzed on a standard laboratory salinity meter.

DT-2851 frame grabber

57. The DT-2851 is a 512- × 512- × 8-bit frame grabber for real-time digital image processing on the IBM-PC/AT-compatible microcomputers. The DT-2851 is a board that installs into a microcomputer and digitizes a video signal, stores an image in one of two onboard memory buffers, and displays the image in color or monochrome at a rate of up to 30 frames per second. The DT-2851 can accept color or monochrome video input from an ordinary video camera or solid-state camera and is also compatible with video input from video cassette recorder (VCR) tape. Image processing software called DT-IRIS is available for use with the DT-2851 and allows the user to perform operations on captured video images using FORTRAN, C, or PASCAL languages. Before a microcomputer can manipulate and enhance an image, it must acquire the image from a camera or other source. Most video devices, i.e., video cameras and VCR's, conform to either the RS-170 or the National Television System Committee (NTSC) standard for 60-Hz television systems, or to the International Radio Consultative Committee (CCIR) or the phase-alternation-line (PAL) standard for 50-Hz systems. The RS-170 signals contain lines of black-and-white (monochrome) video and synchronization timing data. NTSC signals provide the same intensity and sync data as the RS-170 signal, but they contain color information as well.

58. Ordinary VCR's provide an inexpensive and convenient means for storing images for later processing. Unfortunately, most low-cost VCR's are not high-grade engineering tools. Consequently, the VCR's NTSC signal may produce good television images; however, they are often too poor to accurately

trigger the timing circuits on many frame grabber boards. Therefore, it is recommended that a high-quality VCR compatible with the DT-2851 be used to record the dredged material disposal experiments.

59. Once the dredged material disposal has been recorded on video tape, it can be analyzed using the DT-2851 and specially developed software to determine the fall velocity of the sediment cloud during the convective descent phase, the rate at which the cloud expands during convective descent, the change in the cloud's size and shape during descent, and the rate of bottom spreading during dynamic collapse. In order to determine the physical dimensions of the cloud, its location in three-dimensional space, and its descent velocity, the principles of photogrammetry will be useful for the laboratory experiments. Two video cameras placed in different locations will take simultaneous pictures of the sediment cloud and a few control points with accurately known positions in the test tank space. The three-dimensional coordinates of the cloud can be determined by calculating the intersection between two rays going from the cameras to the cloud outline. This calculation can be done by microcomputer feed with data read off the DT-2851 pictures in much the same manner as a stereo comparator is used for land surveying. A timing device that displays time to the nearest 0.01 sec, preferably one that can record directly through the video camera onto the video tape, will also be needed to synchronize processing of the recorded video images from the two cameras.

60. Measurement of eddy velocities induced in the ambient fluid by the descending sediment cloud may be possible by adding a neutrally buoyant tracer (such as puffs of fluorescent dye or small Perspex particles) to the ambient waters prior to the disposal release. The tracer should be arranged in a three-dimensional grid pattern throughout the region of anticipated cloud descent. As the sediment cloud descends, the tracer will tend to follow the movement of the ambient waters and will be recorded on video for later processing.

61. As an option a third video camera can be mounted overhead to monitor the disposal experiment from above. This angle may provide useful information regarding the shape of the cloud as it descends through the water column and as it spreads on the bottom during the dynamic collapse phase. It may be necessary to outfit the camera with a polarizing filter to remove glare from the water surface.

OBS-2 turbidimeter

62. The OBS-2 is an optical backscatter device that measures suspended solids concentrations and turbidity in water by detecting the radiation scattered by suspended matter at angles greater than 90 deg. The theory of light scatter and adsorption by suspended particles is presently not adequate to allow for direct determination of particle concentrations using optical instruments. Therefore, it will be necessary to calibrate the OBS-2 with suspended sediments to be used in the model experiments. Because of its small size (5 cm by 1.8 cm), the OBS-2 sensor is well-suited for use in the proposed laboratory experiments. This will cause minimal disturbance to the flow field created by the descending disposal cloud. The required sample volume is also small (less than 20 ml), which allows the OBS-2 sensor to resolve fine spatial gradients of particle concentrations and turbidity. The OBS-2 can accommodate up to five sensors. An OBS-2 sensor consists of a high-intensity infrared-emitting diode, a detector comprised of four silicon photodiodes, and a linear solid-state temperature transducer. The detector is shielded from visible light by a gelatin filter with a transmittance of less than 1 percent at a wavelength less than 790 nm (1 nm = 10^{-9} m). The OBS-2 sensor responds linearly to sediment concentrations spanning four orders of magnitude, which makes it well-suited for measuring the descending cloud concentration as it varies with time and location.

63. The instrument can measure sand sediment concentrations from 100 mg/ℓ up to 100,000 mg/ℓ. The preliminary DIFID model runs indicated maximum expected concentrations of the sediment cloud at the end of dynamic collapse to be roughly on the order of 50,000 mg/ℓ for all cases except for a few of the large 4,000-yd^3 dumps, which were above 100,000 mg/ℓ. Thus, the OBS-2 should be able to measure nearly the entire range of suspended sediment concentrations anticipated for the dredged material disposal tests. An array of five OBS-2 sensors should be arranged in the test tank. For a disposal into quiescent water, three sensors could be arranged along the vertical center line of the disposal descent and the other two on the bottom radially outward from the center point of the bottom impact area.

Laser-Doppler velocimeter

64. The laser-Doppler technique has been used quite successfully for measuring velocities in homogeneous fluids. The technique does not distort the flow field and requires no calibration; thus, it is particularly

attractive for use in sediment-laden flows. In homogeneous fluid flows, the laser-Doppler technique depends on the presence of small particles that scatter the laser light. The flow must either be seeded (i.e., particles added to the fluid) or filtered to obtain a diffuse distribution of existing scattering particles. Ideally, only one particle at any instant in time should be pres-ent in the measuring volume. The tracer particles should be small (about 10 microns in diameter) to follow the small scale of the fluid flow. For the laser-Doppler technique to be useful in a sediment-laden flow, such as will be experienced in the dredged material disposal tests, the light scattered by the fluid tracer particles must be detectable and distinguishable from that scat-tered by the sediment grains. The measuring volume must be such that the sediment grains appear diffuse; in other words, there are times in which only a fluid tracer particle is in the measuring volume (van Ingen 1981).

65. The adaptation of the laser-Doppler equipment involves the use of a dual-scattering optical arrangement in which the laser light beam is split into two beams of equal intensity that are then made to intersect at a point within the flow field. When a particle passes through the beam, it scatters light from both beams simultaneously at a frequency shifted according to the Doppler principle. The combined light scattered from both beams is collected by a photodetector, which generates an output current that is proportional to the square of the intensity of the incident light.

66. The preliminary DIFID model runs have indicated that the sediment cloud at the end of bottom collapse will have maximum sediment concentrations of about 50,000 mg/ℓ. Thus, the laser-Doppler technique will not be applicable to the portion of the cloud having these high concentrations. However, it may be possible to use the technique to measure fluid movement at the fringes of the sediment cloud where concentrations are relatively low. Other possible problems in using the laser-Doppler velocimeter may be encountered due to the length that the laser beam must pass through the test tank. Most laboratory experiments using the laser-Doppler equipment are conducted with flumes having widths on the order of 1 to 2 ft. The width of the proposed tank is 30 ft.

Suspended sediment sampling

67. Collection of suspended sediment concentrations by manual sampling techniques should also be employed as a means of supplementing and "ground-truthing" the measurements made by the OBS-2 instrument. A three-dimensional

grid consisting of a number of 1/8-in.-diam tubes can be arranged in the testing tank. Small water samples would be collected using a vacuum system that would draw water and sediment from the descending cloud and bottom spreading phase into test tubes for analysis. Timing will be somewhat tricky for capturing a representative sample of the descending sediment cloud and will probably involve some fine-tuning by trial and error. Sampling via the vacuum system can be automatically controlled by signals from the microcomputer.

Barge and pipeline disposal control

68. The release of dredged material from the barge or pipeline can be controlled automatically by the microcomputer and data acquisition and control adapter. The model barge disposal operation may involve opening several compartments at specific time intervals to closely match disposal practices found in the prototype. A signal from the microcomputer at the precise moment will trigger the barge compartment to open and release the dredged material. This trigger signal will also start data collection at all model sensors and can even prompt the video cameras to begin filming. The microcomputer can also be instructed to send control signals to a servomechanical motor/pulley assembly to set the speed of the barge for towed barge experiments. A simple variable-speed motor operating a notched gear with a matching chain attached to the barge can control the movement of the barge.

Establishing a density gradient

69. It may be possible to establish an ambient water density gradient in the test sump by initially filling the sump with layers of salt water having different densities. To keep the different layers from mixing during the filling process, it is recommended that large sheets of plastic or other synthetic material be used to separate the layers. First the bottom layer is filled with the highest salinity water. Then a synthetic sheet covering the entire plan view area of the sump is placed on top of the water. The next higher salinity water is then pumped on top of the synthetic sheet to form another layer. This process is repeated until the desired number of layers (i.e., desired density gradient) is achieved. Prior to the start of a model test, the synthetic sheets will be carefully removed onto rollers at the end of the test tank and the various test monitoring equipment can then be lowered into position.

Data Acquisition and Management

70. The equipment and software that handle the data for model control and data processing can be configured in a variety of ways, each with its unique advantages and disadvantages. Presented in this section is a general description of one possible configuration for the test facility. Discussion with WES personnel indicates that some (or all) of the necessary hardware may already exist at WES.

71. The dredged material disposal test facility will be outfitted with a microcomputer-based data acquisition and control system for acquiring information from the various electronic sensors during the course of model testing. A standard IBM-AT-compatible (or 80386 processor) microcomputer can be used for this purpose. Interfacing of the microcomputer with the electronic sensors will be accomplished through a data acquisition and control adapter and associated software. The adapter will allow the following functions to be performed:

a. Convert analog signals from sensors to digital signals that can be transmitted to the microcomputer.

b. Convert digital signals from the microcomputer to analog signals that can be used as input signals to the control elements in the test facility.

c. Convert digital signals from the microcomputer to discrete contact closures for on/off control functions.

d. Convert switch closures to digital signals that can be transmitted to the microcomputer.

e. Electrically isolate signals from digital sensors and process the signals for transmission to the microcomputer.

f. Provide electrically isolated logic levels to digital control elements.

A variety of adapter cards are available for the IBM-AT so almost any conceivable sensor or control element can be interfaced. The microcomputer must also be equipped with a hard disk to allow for file storage of test data. Figure 8 illustrates a data management system with a single microcomputer handling both on-line data acquisition and control and off-line data processing.

72. Control software will be written in a convenient language (e.g., FORTRAN, PASCAL, C, etc.) that will access each channel of the data acquisition adapter and store the values in the disk file. Each file record will be tagged with date, time, and channel number. Associated with each test data

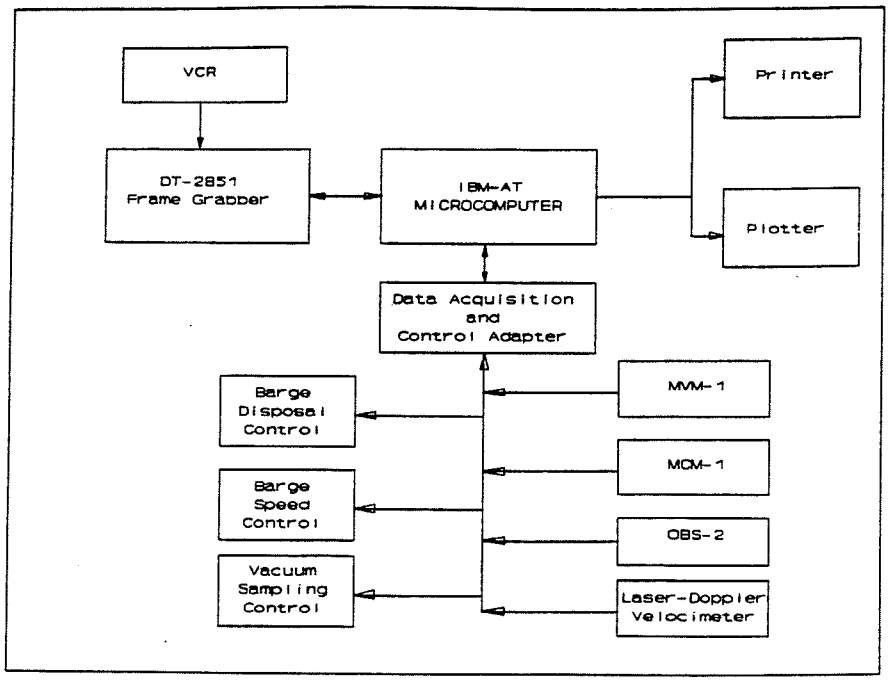

Figure 8. Microcomputer-based data management system

file may be various auxiliary files that contain calibration coefficients to be applied to each of the model sensors. Data acquisition sampling time will be roughly at intervals of 0.1 sec; in other words, a data value will be collected from each model sensor 10 times every second and stored in a data file record. Assuming a 1:100 linear scale model with a 1:10 time scale and a prototype time to end of dynamic collapse of 1,200 sec (based on the preliminary DIFID model runs), the total time for a dredged material disposal test will be about 120 sec. Thus, if data are collected from 20 channels of the data acquisition adapter, then the file record size will consist of integer values for month, day, year, hour, minute, a real value for seconds, and 20 integer data values for a total record size of 54 bytes. The total data file size for a single test will be about 65,000 bytes based on this scenario.

PART IV: CONCLUSIONS AND RECOMMENDATIONS

Conclusions

73. The fundamental question concerning dredged material disposal modeling tests is what, if any, aspects of the laboratory tests can be scaled to the prototype? This report has presented a detailed analysis to determine the applicable scaling laws pertinent to modeling of dredged material disposal releases into coastal and estuarine waters. It is concluded that physical model studies can be reasonably and accurately scaled to prototype phenomena and results from such model studies will increase the scientific knowledge of the physical processes that occur during the open-water disposal of dredged material. The following conclusions are made regarding physical model experiments for dredged material disposal:

a. According to the dimensional analysis presented in Part II of this report, reasonably accurate simulation of sediment cloud convective descent and dynamic collapse can be obtained as long as the model Reynolds number is high enough. Although absolute flow Reynolds number similitude in the water column cannot be achieved, keeping the model Reynolds number greater than 10^3 will maintain the coefficient of drag at approximately the same magnitude as would be found in the prototype where the Reynolds number is much greater than 10^3 (Figure 1). Thus, the effects of drag on the convective descent will be similar in both model and prototype.

b. Assuming that dynamic collapse occurs on the bottom, it is necessary that model and prototype Reynolds number similitude be achieved. It has been shown that this is possible by increasing the bottom sediment diameter.

c. The Reynolds number requirements put a limit on the model-to-prototype scale ratios that can be used. The flow Reynolds number in the model at the beginning of either convective descent or dynamic collapse should be high enough to cause turbulent flow. This places a limit on the smallest scale that can be used for modeling the dredged material disposal processes at 1:100. In other words, the physical model scale will need to be greater than or equal to 1:100 (e.g., 1:75, 1:50, etc.).

d. Cohesive sediments in the form of clumps that do not break up during either convective descent or dynamic collapse can be assumed to behave in the same manner as noncohesive particles for the model experiments. Scale effects on particle settling are more important for a dynamic collapse that occurs in the water column (which rarely occurs in the prototype) than for bottom collapse phenomena.

e. Most likely the numerical model formulations in such models as

DIFID, DMF, and DMFJ will need to be modified to treat cohesive sediments and bottom collapse phases based on results from the physical model experiments.

f. Existing monitoring equipment and sump facilities at WES can be used for much of the hardware required for constructing the test facility, thus reducing the cost.

Recommendations

74. It is recommended that initial dredged material model tests be kept simple; that is, they should be stationary disposals into nonstratified waters with noncohesive materials. This will allow the scientists and engineers to test the assumptions of the scaling analysis presented in this report, and will enable them to determine the best use of monitoring methods and equipment. Then when the physics of the scale model are better understood, more complex tests can be conducted including moving discharges, pipeline jet disposal, and stratified receiving waters, among others.

75. It is also recommended that more consideration be given to the construction costs involved in modifying the Georgetown Harbor sump for the test facility and to the costs of monitoring equipment. The following are approximate costs for the monitoring equipment described in Part III of this report.

a.	MVM-1 velocity meter	$ 2,000.00
b.	MCM-1 salinity meter	2,000.00
c.	OBS-2 turbidimeter	7,500.00
d.	DT-2851 frame grabber	2,995.00
e.	DT-IRIS image processing software	995.00
f.	Laser-Doppler velocimeter	15,000.00
g.	IBM-AT compatible microcomputer	2,500.00

REFERENCES

Bowers, G. R., and Goldenblatt, M. K. 1978. "Calibration of a Predictive Model for Instantaneously Discharged Dredged Material," EPA-600/3-78-089, US Environmental Protection Agency, Corvallis Environmental Research Laboratory, Corvallis, OR.

Brandsma, M. G., and Divoky, D. J. 1976. "Development of Models for Prediction of Short-Term Fate of Dredged Material Discharged in the Estuarine Environment," Contract Report D-76-5, US Army Engineer Waterways Experiment Station, Vicksburg, MS.

Brandsma, M. G., Ayers, R. C., Jr., and Sauer, T. C., Jr. 1983. "Mud Discharge Model, Report and User's Guide, Model Version 1.0," Exxon Production Research Company.

Ditmars, J. D., and McCarthy, M. J. 1975. "Particle-Laden Jets with Application to Ocean Dumping," Symposium on Modeling Techniques, American Society of Civil Engineers, New York, Vol 1, pp 335-351.

Dyer, K. R. 1986. Coastal and Estuarine Sediment Dynamics, Wiley, New York.

Fischer, H. B. 1972. "A Numerical Model of Estuarine Pollutant Transport," Proceedings of the 13th Coastal Engineering Conference, American Society of Civil Engineers, New York, pp 2265-2274.

Fischer, H. B., List, E. J., Koh, R. C. Y., Imberger, J., and Brooks, N. H. 1979. Mixing in Inland and Coastal Waters, Academic Press, New York.

Graf, W. H. 1971. Hydraulics of Sediment Transport, McGraw-Hill, New York.

Johnson, B. H., Holliday, B. W., and Thomas, W. A. 1978. "Predicting and Monitoring Dredged Material Movement," Technical Report DS-78-3, US Army Engineer Waterways Experiment Station, Vicksburg, MS.

Johnson, B. H. "User's Guide for Models of Dredged Material Disposal in Open Water" (in preparation). US Army Engineer Waterways Experiment Station, Vicksburg, MS.

Koh, R. C. Y., and Chang, Y. C. 1973. "Mathematical Model for Barged Ocean Disposal of Waste," EPA-660/2-73-029, US Environmental Protection Agency, Office of Research and Development, Washington, DC.

Muellenhoff, W. P., Soldate, A. M., Jr., Baumgartner, D. J., Schuldt, M. D., Davis, L. R., and Frick, W. E. 1985. "Initial Mixing Characteristics of Municipal Ocean Discharges; Vol I, Procedures and Applications," EPA-600/3-85-07-03a, Pacific Division Environmental Research Laboratory, Narragansett Office of Research and Development, US Environmental Protection Agency, Newport, OR.

Schlichting, H. 1968. Boundary Layer Theory, McGraw-Hill, New York.

Sleath, J. F. A. 1984. Sea Bed Mechanics, Wiley, New York.

Tetra Tech. 1982. "Evaluation of Ocean Disposal of Manganese Nodule Processing Waste and Environmental Considerations," prepared for National Oceanic and Atmospheric Administration, Office of Ocean Minerals and Energy, Washington, DC, and US Environmental Protection Agency, Criteria and Standards Division, Washington, DC.

Turner, J. S. 1986. "Turbulent Entrainment: The Development of the Entrainment Assumption, and Its Application to Geophysical Flows," Journal of Fluid Mechanics, Vol 173, pp 431-471.

van Ingen, C. 1981. "Observations in a Sediment-Laden Flow by Use of Laser-Doppler Velocimetry," Report No. KH-R-2, W. M. Keck Laboratory of Hydraulics and Water Resources, California Institute of Technology, Pasadena, CA.

Table 1

Summary of Results of Preliminary DIFID Model Runs

Disposal Volume yd^3	Water Depth ft	Sediment Cloud Diameter ft	Maximum Concentration mg/ℓ	End Time sec*	Depth to Top of Cloud ft**	DIFID Run Codes† v	d	b	s	p	w
200	100	373	49,159	324	--	1	1	1	3	1	4
200	300	805	10,704	960	|	1	2	1	3	1	3
200	500	1,127	2,883	1,526	|	1	3	1	3	1	3
200	700	1,413	1,350	2,105	|	1	4	1	3	1	3
					|					
500	100	432	115,146	241	|	2	1	1	3	2	4
500	300	918	18,574	926	|	2	2	1	3	1	3
500	500	1,271	6,130	1,421	|	2	3	1	3	1	3
500	700	1,589	2,790	1,932	|	2	4	1	3	1	3
					|					
1,000	100	467	320,131	183	|	3	1	1	3	3	2
1,000	300	1,022	34,902	908	|	3	2	1	3	1	3
1,000	500	1,395	10,391	1,368	|	3	3	1	3	1	3
1,000	700	1,740	5,083	1,827	|	3	4	1	3	1	3
					|					
2,000	100	510	202,812	146	|	4	1	1	3	2	5
2,000	300	994	29,866	686	|	4	2	1	3	1	4
2,000	500	1,544	17,718	1,332	|	4	3	1	3	1	3
2,000	700	1,910	8,456	1,760	|	4	4	1	3	1	3
					|					
3,000	100	563	259,126	152	|	5	1	1	3	2	5
3,000	300	1,064	41,235	680	|	5	2	1	3	1	4
3,000	500	1,642	26,660	1,318	|	5	3	1	3	1	3
3,000	700	2,023	11,345	1,731	|	5	4	1	3	1	3
					|					
4,000	100	595	328,082	142	|	6	1	1	3	4	5
4,000	300	1,076	58,859	479	|	6	2	1	3	2	4
4,000	500	1,718	34,001	1,311	|	6	3	1	3	1	3
4,000	700	2,108	14,109	1,709	↓	6	4	1	3	1	3

* Time to end of dynamic collapse phase in seconds.

** For all these cases, DIFID computed the cloud to be completely on the bottom.

† DIFID Run Codes denote input parameters as follows:

v = disposal volume (yd^3)

1 = 200
2 = 500
3 = 1,000
4 = 2,000
5 = 3,000
6 = 4,000

d = water depth (ft)

1 = 100
2 = 300
3 = 500
4 = 700

b = bulk density (g/cm^3)

1 = 1.5

s = barge speed (knots)

1 = 0.0
2 = 2.0
3 = 4.0

p = ambient density gradient, (g/cm^3)

1 = 0.00000000
2 = 0.00000143
3 = 0.00000286
4 = 0.00000429

w = settling velocity (fps)

1 = clumps	= 0.50000
2 = clay	= 4.0E-04
3 = silt	= 8.0E-03
4 = fine sand	= 3.0E-02
5 = medium sand	= 8.0E-02

Table 2

Effect of Length Scale Ratio on Model Depth and Sediment Cloud Size

Prototype			Model:Prototype Scales			Model		
Water Depth ft	Maximum Cloud Diameter ft	Barge Speed knots	Length Scale	Time Scale	Velocity Scale	Water Depth ft	Bottom Cloud Major Axis Length ft	Bottom Cloud Minor Axis Length ft
700	2,108	4.0	1:100	1:10	1:10	7.0	37.3	21.1
	2,103	2.0	1:100	1:10	1:10	7.0	29.2	21.0
	2,099	0.0	1:100	1:10	1:10	7.0	21.0	21.0
	2,108	4.0	1:81	1:9	1:9	8.64	46.1	26.0
	2,103	2.0	1:81	1:9	1:9	8.64	36.0	26.0
	2,099	0.0	1:81	1:9	1:9	8.64	25.9	25.9
	2,108	4.0	1:75	1:8.66	1:8.66	9.33	49.9	28.1
	2,103	2.0	1:75	1:8.66	1:8.66	9.33	38.9	28.0
	2,099	0.0	1:75	1:8.66	1:8.66	9.33	28.0	28.0
500	1,718	4.0	1:100	1:10	1:10	5.0	33.5	17.2
	1,711	2.0	1:100	1:10	1:10	5.0	25.3	17.1
	1,709	0.0	1:100	1:10	1:10	5.0	17.1	17.1
	1,718	4.0	1:75	1:8.66	1:8.66	6.67	44.7	22.9
	1,711	2.0	1:75	1:8.66	1:8.66	6.67	33.7	22.8
	1,709	0.0	1:75	1:8.66	1:8.66	6.67	22.8	22.8
	1,718	4.0	1:50	1:7.07	1:7.07	10.0	67.0	34.4
	1,711	2.0	1:50	1:7.07	1:7.07	10.0	50.5	34.2
	1,709	0.0	1:50	1:7.07	1:7.07	10.0	34.2	34.2
300	1,076	4.0	1:100	1:10	1:10	3.0	27.1	10.8
	1,070	2.0	1:100	1:10	1:10	3.0	18.9	10.8
	1,069	0.0	1:100	1:10	1:10	3.0	10.7	10.7
	1,076	4.0	1:75	1:8.66	1:8.66	4.0	36.1	14.4
	1,070	2.0	1:75	1:8.66	1:8.66	4.0	25.2	14.3
	1,069	0.0	1:75	1:8.66	1:8.66	4.0	14.2	14.2
	1,076	4.0	1:50	1:7.07	1:7.07	6.0	54.2	21.5
	1,070	2.0	1:50	1:7.07	1:7.07	6.0	37.7	21.4
	1,069	0.0	1:50	1:7.07	1:7.07	6.0	21.4	21.4
100	595	4.0	1:100	1:10	1:10	1.0	22.3	6.0
	589	2.0	1:100	1:10	1:10	1.0	14.0	5.9
	586	0.0	1:100	1:10	1:10	1.0	5.9	5.9
	595	4.0	1:50	1:7.07	1:7.07	2.0	38.6	11.9
	589	2.0	1:50	1:7.07	1:7.07	2.0	28.1	11.8
	586	0.0	1:50	1:7.07	1:7.07	2.0	11.7	11.7
	595	4.0	1:25	1:5	1:5	4.0	89.1	23.8
	589	2.0	1:25	1:5	1:5	4.0	72.5	23.6
	586	0.0	1:25	1:5	1:5	4.0	23.4	23.4

Notes: The model bottom cloud major axis length was computed assuming a disposal from a barge having four compartments released at 1-min (60-sec) intervals. The resulting bottom cloud is assumed to be the superposition of the four individual instantaneous releases and is considered to be a conservative value.
Disposal volume was 4,000 yd^3.

APPENDIX A: NOTATION

a	Entrainment coefficient
A	Dimensionless parameter in Buckingham pi method
b	Radius of disposal cloud at time > 0 (L)
b_0	Radius of disposal cloud at time of release (L)
C	Concentration (M/L^3)
C_D	Coefficient of drag
d	Water depth
d_I	Diameter of sediment cloud upon impact with seafloor (L)
D	Particle grain diameter (L)
D_b	Mean bottom sediment diameter (L)
g	Acceleration of gravity (L/T^2)
g'	$g\left[\rho_0 - \rho_a(0)\right]/\rho_1$ (L/T^2)
h_0	Initial height of bottom cloud (L)
J	Number of solid particle types
k	Physical dimension in Buckingham pi theorem
k_s	Bed roughness (L)
L	Length
L_R	Model-to-prototype length scale ratio
m	Subscript denoting model physical and dimensionless parameters
M	Mass
n	Exponent
N	Brunt-Vaisala frequency, or buoyancy (L/T)
q_i	Physical quantity in Buckingham pi theorem
r_0	Initial radius of bottom cloud (L)
R	Radius of cloud
Re	Reynolds number
S_a	Initial dilution of sediment cloud upon impact with seafloor
t	Time (T)
t_I	Time required for cloud to completely impact seafloor (T)
T	Time
T_R	Model-to-prototype time scale ratio
u	Ambient water current velocity (L/T)
u_B	Barge speed (L/T)

u_*	Shear velocity (L/T)
U_0	Initial radial speed of bottom cloud spreading (L/T)
V_j	Total volume of particles of each grain diameter
w	Fall velocity of sediment cloud (L/T)
w_0	Initial fall velocity of disposal cloud (L/T)
w_c	Concentration-dependent fall velocity (L/T)
w_I	Fall velocity of sediment cloud upon impact with seafloor (L/T)
w_j	Fall velocity of j^{th} particle (L/T)
W	Spherical particle fall velocity (L/T)
z	Depth (L)
z_0	b(t)/a
Z_0	Bed roughness height (L)
β	Constant relating particle fall velocity to concentration
ν	Kinematic viscosity (L^2/T)
π_i	Dimensionless group in Buckingham pi theorem
ρ	Bulk density (M/L^3)
ρ_0	Initial bulk density (M/L^3)
ρ_1	Reference density in the environment (M/L^3)
$\rho_a(z)$	Density of receiving water at depth z (M/L^3)
ρ_b	Bed particle density (M/L^3)
ρ_I	Bulk density of sediment cloud upon impact with seafloor (M/L^3)
ρ_s	Particle density (M/L^3)

Waterways Experiment Station Cataloging-in-Publication Data

Soldate, Mills.

Preliminary design for dredged material placement physical modeling facilities / by Mills, Soldate, James R. Pagenkopf, Michael R. Morton, Tetra Tech, Inc. ; prepared for Department of the Army, US Army Corps of Engineers ; monitored by Hydraulics Laboratory, U.S. Army Engineer Waterways Experiment Station.

55 p. : ill. ; 28 cm. — (Technical report ; DRP-92-8)

Includes bibliographical references.

1. Dredging spoil — Environmental aspects. 2. Sediment transport — Testing. 3. Diffusion in hydrology — Testing — Models. 4. Hydraulic models. I. Pagenkopf, James R. II. Morton, Michael R. III. United States. Army. Corps of Engineers. IV. Tetra Tech, inc. V. U.S. Army Engineer Waterways Experiment Station. VI. Dredging Research Program. VII. Title. VIII. Series: Technical report (U.S. Army Engineer Waterways Experiment Station) ; DRP-92-8.

TA7 W34 no.DRP-92-8